UNRAVELLING THE MYSTERIES OF COGNITIVE DECLINE IN CANCER SURVIVORS USING FUNCTIONAL NEAR INFRARED SPECTROSCOPY

by

DHIVYA SRINIVASAN

1001234963

Presented to the Faculty of Graduate School of

The University of Texas at Arlington in Partial Fulfillment

Of the Requirements

For the Degree of

MASTER OF SCIENCE IN BIOENGINEERING

THE UNIVERSITY OF TEXAS AT ARLINGTON

May 2017

Acknowledgements

First and foremost, I would like to extend my profound gratitude to my advisor, Professor Dr.Hanli Liu, for her considerate guidance, affectionate attitude & motivation. Throughout this learning curve and experimentation, she has been an unfaltering pillar of expertise, encouragement & inspiration. I am truly grateful for all the facilities and knowledge I gained during this journey from Dr. Liu. To Dr. Liu, thank you for untiring support and for introducing me to innovative ideas that has made me what I am now.

With great regard, I wish to thank my committee members, Dr. Pascal Jean-Pierre, Dr. Suvra Pal and Dr. Liu, for accepting to be a part of my thesis defense committee, for their valuable inputs & for their precious time. I would like to thank Dr. Tian Fenghua for his support and inputs in achieving results. I owe special thanks to Dr. Pal for spending time in making me to understand Statistical Concepts in short span and Dr.Pascal for the data.

Besides, I would like to express my special thanks to my lab mate Harish for constantly working with me & for his suggestions at various levels of project. I would also thank all my lab colleagues especially Amarnath, Ola & Xinlong for their support, training & for sharing their knowledge. I take the opportunity thank all my friends for their timely motivation, emotional support & unfailing help by all means during the entire course of study.

I may short fall of words in expressing my sincere gratitude to my Father Mr. Srinivasan and my mother Mrs. Padma Srinivasan and sisters for all the emotional, moral & financial support they have given to me throughout my life. Finally, I would like to extend my heartfelt thanks to one last person Dhinesh, for being with me and for pushing me forward to reach my goals.

May 04,2017

Abstract

UNRAVELLING THE MYSTERIES OF COGNITIVE DECLINE IN CANCER SURVIVORS USING FUNCTIONAL NEAR INFRARED SPECTROSCOPY

Dhivya Srinivasan, M.S.

The University of Texas at Arlington, 2017

Supervising Professor: Dr. Hanli Liu

In recent years, there has been an increased incidence of cognitive impairment in cancer survivors as a side-effect of chemotherapy. This troubling deterioration in cognitive ability is commonly termed as 'Chemo brain' in which patients have problems with working memory, executive function, decision-making, concentration, visuospatial skills and attention which can pose problems to get on with day-to-day life. Breast Cancer is primarily adopted as the model for studying effects of 'chemobrain'. A better understanding of neural correlates & hemodynamic changes related to cognitive deficits would help clinicians to design targeted treatments and cognitive rehabilitation interventions.

Aim: The primary goal of this study is to investigate the feasibility of using functional near infrared spectroscopy (fNIRs) to monitor hemodynamic changes in prefrontal cortex induced by certain neuropsychological tests in cancer survivors and to identify a possible biomarker for cognitive decline.

Method: 15-healthy control subjects grouped into two consisting of 9 young adults (age group: 15-21), 6 elderly adults (age group: 40-74) & 3 cancer patients (age group: 30-50) participated in this study. Hemodynamic changes during different neurocognitive tests like go/no-go, stroop, n-back working memory with different cognitive loads were measured using 16-channel near infrared spectroscopy (fNIRs) system.

Results: Cancer patients have shown deactivation in VLPFC because of cognitive decline and right VLPFC could be a possible biomarker for studying cancer related changes. In both young and elderly adults, pre-frontal activation increased with increasing work-memory load for n-back test. There is slight right hemispheric dominance observed in young adults for low memory load condition but elderly subjects recruit both the hemispheres in attempt to compensate for age-related decline in performance. For Go/No-Go task, we can see diffuse and bilateral patterns of activation in in ventrolateral Prefrontal Cortex(VLPFC) for elderly adults.

Conclusion: These results support the previous findings that prefrontal cortex plays a key role in executive functions with varying working memory load and fNIRS can be used as potential tool to study cognitive changes. It provides further evidence that PFC activation/deactivation could be a possible neuro-functional biomarker for monitoring executive impairment associated with chemo brain (chemotherapy -treated cancer survivors).

Table of Contents

Acknowledgments..... ii

Abstract iii

List of Figures viii

List of Tables x

List of Abbreviation xi

CHAPTER 1 INTRODUCTION 1

1.1 Functional Near Infrared Spectroscopy 1

1.1.1 Blood Chromophores & Absorption spectra 2

1.1.2 Principle of Brain Imaging using Near Infrared Light 2

1.1.3 Light Propagation in Biological Tissue 3

1.1.4 Beer Lambert's Law & MBLL 5

1.1.5 fNIRS Instrumentation 8

1.1.5.1 CW-NIRs 9

1.1.5.2 Time-Domain NIRs 10

1.1.5.3 Frequency-Domain NIRs 10

1.2 Physiology of Hemodynamic Response & Neuronal Activity..... 11

1.3 Neurophysiology of Prefrontal Cortex 13

1.4 Cancer Related Neurocognitive Dysfunction..... 15

1.4.1 Chemo brain 16

1.4.2 Mechanisms of CRND 17

1.4.3 Clinical Characteristics of CRND 19

1.5 Focus of this Study 20

1.6 Outline of this study 21

CHAPTER 2 METHODOLOGY 22

2.1 Selection of Subjects 22
2.2. Instrumentation 23
2.2.1 fNIRS system 23
2.3 Protocol/ Experimental Paradigm 25
2.3.1 N-back Test 25
2.3.2 Go/No-Go Task 26
2.3.3 Stroop Task 27
2.4 Data Analysis 29
2.4.1 Data Screening & Pre-Processing 29
2.4.2 General Linear Model 30
2.4.3 Topographical Plots 31
2.4.4 Statistical Analysis 32
2.4.4.1 Linear Mixed Effect Model 32
2.4.4.2 Two-sample t-tests 33
CHAPTER 3 RESULTS 34
3.1 Hemodynamic Responses 35
3.1.1 Hemodynamic Response: N-back Test 36
3.1.1.1 Healthy Old Vs Healthy Young 36
3.1.1.2 Cancer Vs Healthy Old 37
3.1.2 Hemodynamic Response: Go/No-Go Test 39
3.1.2.1 Healthy Old Vs Young 40
3.1.2.1 Cancer Vs Healthy Old 40
3.1.3 Hemodynamic Response: Stroop Test 42
3.1.3.1 Healthy Old Vs Young 42
3.1.3.2 Cancer Vs Healthy Old 43
3.2 Statistical Results: Linear Mixed Model 45
3.2.1 N-Back Test 46
3.2.2 Stroop Test 47

3.2.3 Go/No-Go Test.....47
CHAPTER 4 DISCUSSION & FUTURE WORK 48
4.1 Discussion 48
4.2 Limitations 51
4.3 Future Work 51
REFRENCES 53

LIST OF FIGURES

Figure 1: Absorption Spectra of Chromophores and Optical Window 1
Figure 2: Banana path of light with Source and detector 2
Figure 3: At different source-detector separation 3
Figure 4: Light Propagation in Biological Tissue 3
Figure 5: Photon-Tissue Interaction 4
Figure 6: Beer-Lamberts Law 5
Figure 7: Modified Beer Lamberts Law 7
Figure 8: Types of fNIRs light transmission 9
Figure 9: Continuous wave NIRS 9
Figure 10: Time domain NIRs 10
Figure 11: Frequency domain NIRs 10
Figure 12: Hemodynamic Response Function 11
Figure 13: Neurovascular Coupling 12
Figure 14: Resting & Activated cerebral Blood Flow 12
Figure 15: Functional Organization of PFC 14
Figure 16: Clinical characteristics- chemo brain 15
Figure 17: Causes for CRND 17
Figure 18: Mechanisms of CRND 18
Figure 19: Symptoms of Chemo brain 19
Figure 20: Demographics in this study 22
Figure 21: Location of Optodes on PFC 23
Figure 22: Arrangement of Sources and Detectors.....24
Figure 23: Experimental Paradigm-N-back 25
Figure 24: Screen for 0-back.....26
Figure 25: Experimental Protocol-Go/No-Go 27
Figure 26: Block Diagram-Go/No-Go 27

Figure 27: Stroop Task 28
Figure 28: Data processing Overall Flow 30
Figure 29: General Linear Model-Regressor.....31
Figure 30: Linear Mixed Effect Model 32
Figure 31: Young Vs Old Hemodynamic Response of n-back 36
Figure 32: Cancer Vs Healthy Hemodynamic Response of n-back 37
Figure 33: Young Vs Old Hemodynamic Response of Go/No-Go 39
Figure 34: Cancer Vs Healthy Hemodynamic Response of Go/No-Go 40
Figure 35: Young Vs Old Hemodynamic Response of Stroop 41
Figure 36: Cancer Vs Healthy Hemodynamic Response of Stroop 42
Figure 37: P-value Plot: Healthy Old Vs Young 43
Figure 38: P-value plot: Cancer Vs Healthy Old 44

LIST OF TABLES

Table 1: Demographics of Younger Adults (18-21) 34
Table 2: Demographics of Older Adults (44-74) 34
Table 3: Demographics of Cancer (30-60) 35
Table 4: Statistical Result: Linear Mixed Effect Model 45
Table 5: Statistical Results: Two Sample t-test 48

LIST OF ABBREVIATIONS

BA- Brodmann Area

BBB- Blood Brain Barrier

BLL- Beer Lamberts Law

BOLD- Blood Oxygen Level Dependent

CBF-Cerebral Blood Flow

CFQ- Cognitive Failure Questionnaire

CICI- Cancer Induced Cognitive Impairment

CNS- Central Nervous System

COBI- Cognitive Optical Brain Imaging

CRND- Cancer Related Neuro Cognitive Dysfunction

CT- Computed Tomography

CW-NIRs- Continuous wave Near Infrared Spectroscopy

DLPFC- Dorsolateral Prefrontal cortex

DMN- Default Mode Network

DNA- De-oxy Ribo Nucleic Acid

DPF- Differential Path length Factor

DTI- Diffuse Tensor Imaging

fMRI-functional Magnetic Resonance Imaging

fNIRS- Functional Near Infrared Spectroscopy

GLM- General Linear Model

HADS- Hamilton Anxiety & Depression Scale

Hb- De-Oxygenated Hemoglobin

HbO- Oxygenated Hemoglobin

HRF-Hemodynamic Response Function

ISI- Insomnia Severity Index for Sleep

LED-Light Emitting Diode

MBLL- Modified Beer Lamberts Law

MFC-Medial Prefrontal Cortex

MRI- Magnetic Resonance Imaging

NCS-Need for Cognition Scale

OD- optical Density

PET- Positron Emission Tomography

PFC- Prefrontal Cortex

SPECT- Single Photon Emission Computed Tomography

TPSF-Temporal Point Spread Function

VLPFC- Ventrolateral Prefrontal Cortex

WM- Working Memory

Chapter 1

Introduction

1.1 Functional Near Infrared Spectroscopy

Functional Near Infrared spectroscopy (fNIRs) is a non-invasive, inexpensive & portable brain imaging technique that measures hemodynamic changes in response to neuronal activation similar to fMRI. The use of fNIRs as a functional imaging technique relies on the principle of neurovascular coupling also known as BOLD response. Through neurovascular coupling, neural activity is linked to changes in local cerebral blood flow. fNIRs works in the wavelength range of 700 – 900 nm, also called as optical window for biological tissues. Visible light with wavelength of 400 – 700 nm is substantially absorbed by intrinsic chromophores such as Hemoglobin, melanin and other components, while at longer wavelengths (> 900 nm) water becomes strong absorber of light. Thus, near-Infrared wavelength region is suitable for optical imaging where the blood has minimal absorbers and strong scatterers.

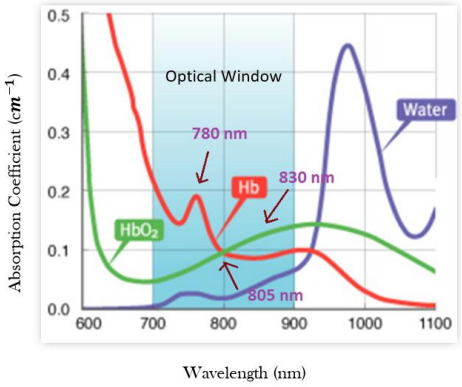

Figure 1: Absorption Spectra of chromophores and optical window

(Source: Practical intravital two-photon microscopy for immunological research: faster, brighter, deeper Tri Giang Phan and Andrew Bullen)

1.1.1 Blood chromophores & Absorption Spectra:

Blood mainly consists of two chromophores namely, oxy-hemoglobin (HbO) which is bound to oxygen and de-oxy Hemoglobin (Hb) is free and does not bound to oxygen. Both the chromophores exhibit different absorption spectra depending on the molar extinction co-efficient of Hemoglobin (Hb). Hemoglobin has its highest absorption peak at 420 nm and second peak at 580 nm and absorption decreases as wavelength increases. The point at which molar extinction coefficient of Hb and HbO intersects is called as isobestic point. So, by utilizing two different wavelengths, one above and one below the isobestic point, we can calculate the relative change in concentration of oxy Hb and de-oxyHb (1).

1.1.2 Principle of Brain Imaging using Near Infrared Light:

fNIRs imaging involves irradiating the surface of head using Near-infrared light via set of optical fibers called as sources. The light, after being absorbed by intrinsic chromophores will diffuse optically (scatter multiple times inside the tissue). It follows banana path while in the process of scattering, reflected back to the surface of head and condensed by set of optical fibers called detectors.

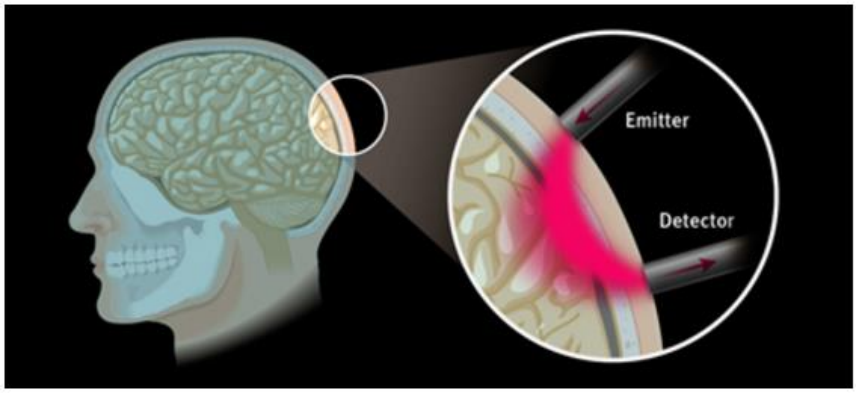

Figure 2: Banana path of light with source and detector

(Source: ISS Imagent)

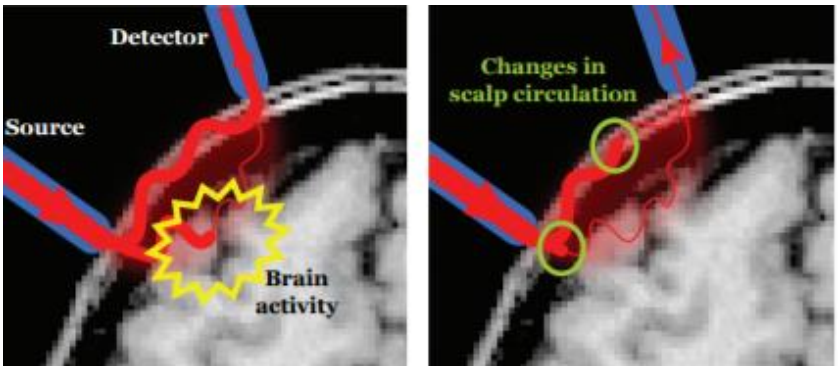

Figure 3: At different source-detector separation

(Source: ISS Imagent)

Thus, the photon exiting the tissue after multiple scattering at a distance of say 3 cm (30 mm) from the source are collected by another optical fiber bundle. Back scattered photons can be detected using detector bundle. The depth and intensity of light penetration depends on the inter optode distance (source- detector separation). In general, greater the source detector separation, deeper the penetration of light (2). However, with increase in source detector separation (fig 3), intensity of light captured by the detector would be low. In contrast, if the distance between the source and the detector is less, then the tissue will not be sampled. Ideally, irrespective of head size, maximum depth of penetration can be achieved with inter-optode distance of 3 cm.

1.1.3 Light Propagation in Biological Tissue:

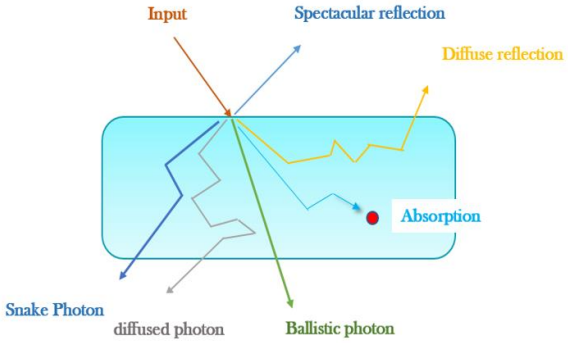

Figure 4: Types of Light interaction with tissue

Photons emitted from NIR source entering the scalp may undergo two types of interaction with tissue.

1. Absorption – absorbed by intrinsic chromophores such as melanin, lipid, water
2. Multiple scattering/Diffusion – scattered many times before reaching the detector

Scattered light will be returned back towards detector or transmitted through the tissue. Some of the injected photons will be lost as a result of scattering and absorption due to different structures in the tissue. Scattering in biological tissue is characterized by its scattering coefficient 'μs'. When photon undergoes multiple scattering events such that they lost the memory of their initial direction of propagation, scattering coefficient becomes reduced scattering coefficient μs' and it is given by,

$$\mu_s' = \mu_s(1 - g) \tag{1.1}$$

where 'g' is the anisotropy factor and it is given by the mean of cosine of scatter angles which takes the value between 0.0 - 1.0.

$$g = \langle cos\,\theta \rangle \tag{1.2}$$

For forward scattering, 'g' takes the value from 0.8 - 1.0. (Source: http://www2.ensc.sfu.ca/~glennc/e376/e376l7.pdf)

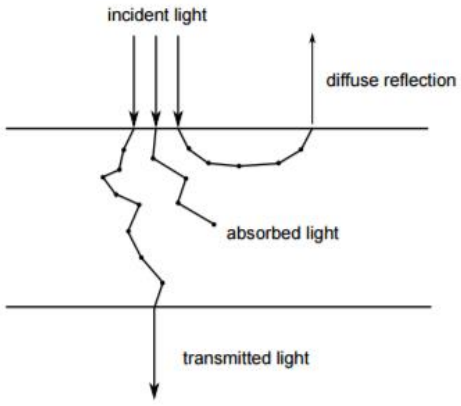

Figure 5: Photon-Tissue Interaction

Tissue's ability to absorb photons is characterized by its absorption coefficient (μ_a). The probability of photon absorption in tissue per unit length is called as Absorption coefficient (μ_a). (1/ μ_a) is referred to as mean absorption length.

Light attenuation in absorption-only medium is given by,

$$I(x) = I_0 \exp(-\mu_a x) \tag{1.3}$$

where 'I' denotes the intensity of light detected by the detector, $'I_0'$ is the initial intensity and

$'x'$ is the optical path length

When the media is diffusive like biological tissue, it permits both absorption and scattering. Total attenuation coefficient μ_t can be written as the sum of μ_a and μ_s:

$$\mu_t = \mu_a + \mu_s \tag{1.4}$$

Light attenuation in diffusive medium is given by,

$$I(x) = I_0 \exp(-\mu_t x) \tag{1.5}$$

1.1.4 Beer Lambert's Law & Modified Beer Lambert's Law (MBLL):

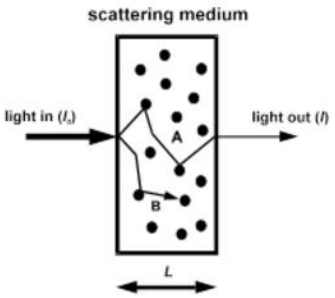

Figure 6: Beer-Lambert's law (Source: Artinis)

For the conversion of raw near-infrared absorption and attenuation intensity data into relative changes in concentration of oxyHb and de-oxyHb, the most commonly used algorithm is Modified Beer-Lamberts Law. The attenuation of light caused by tissue can be related to the concentration of chromophores in tissue by Beer Lambert's Law,

$$I(x) = I_0 \exp(-\mu\, x)$$

where 'μ' explains attenuation by Absorption. In contrast to Beer Lambert's law which accounts for non-scattering media (only absorption), in Modified Beer Lamberts law(MBLL), optical scattering of light will also be considered which is related to chromophore concentration. Scattering of light does not follow straight path in biological tissue but photons exhibit is banana shaped profile. MBLL is an empirical formula to calculate scattered light intensity at the detector using Optical density (OD).

$$OD(\lambda) = \log\left(\frac{I_0}{I}\right) = \mu\, L \qquad (1.6)$$

where OD is the attenuation measures in Optical Densities at particular wavelength of light, I_0 is the initial intensity of light entering the tissue, μ is the attenuation by both absorption and scattering and L is the optical path length.

$$\mu\, L = \varepsilon C L \qquad (1.7)$$

So, eqn(1.6) becomes,

$$OD(\lambda) = \log\left(\frac{I_0}{I}\right) = \mu\, L = \varepsilon C L \qquad (1.8)$$

where ε is the extinction coefficient of absorbing chromophore ($\mu M^{-1}.cm^{-1}$), C is the concentration of chromophore(μM), L is the path length or distance travelled by light between entry and exit points, λ is the wavelength of light.

Blood chromophores Oxygenated Hemoglobin (HbO) and de-oxygenated Hemoglobin (Hb) are the main absorbers of light in NIR region. So Optical density can be quantified as summation of attenuation by both the chromophores.

$$OD(\lambda) = \sum_{i=Hb,HbO} \varepsilon_{i,\lambda} C_i L_\lambda \quad (1.9)$$

where $\varepsilon_{i,\lambda}$ is the extinction coefficient of blood chromophore for wavelength λ.

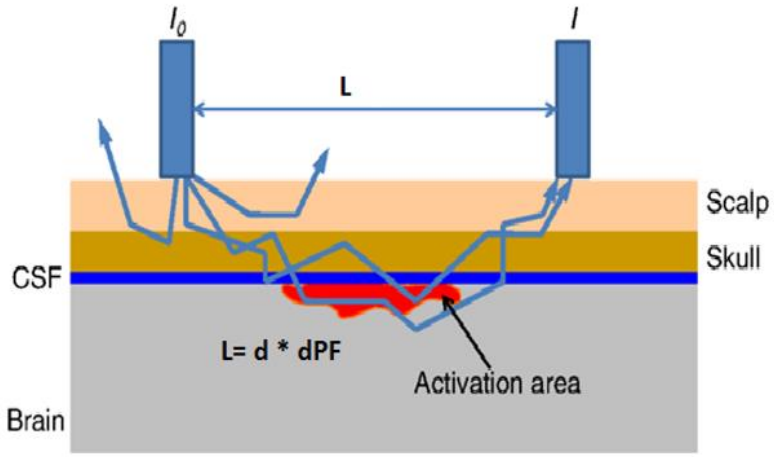

Figure 7: Modified Beer-Lamberts Law

(Source: http://biomedicaloptics.spiedigitallibrary.org/article.aspx?articleid=2534443)

Modified Beer Lambert's law (MBLL) is intended to be used with scattering diffusive medium and hence differential path length correction factor must be included as the path of light will not be perfectly linear in brain. Differential path length factor (DPF) accounts for increase in optical path length dur to multiple scattering in tissue.

$$L_\lambda = \mathrm{d}.DPF_\lambda \quad (1.10)$$

Where d is the distance between source and detector DPF is the differential path length factor which is the correction in the mean photon path length for scattering and is given by,

$$DPF_\lambda = \frac{1}{2}\left[\frac{3\mu_s'}{\mu_a}\right]^{1/2}\left[1 - \frac{1}{1+d.(3\mu_s'\mu_a)^{1/2}}\right]^{1/2} \quad (1.11)$$

When scattering differential path length factor is assumed to be constant for particular wavelength, and hence relative change in concentration is given by,

$$\Delta OD = \sum_{i=Hb,HbO} \varepsilon_{i,\lambda}\, \Delta C_i L_\lambda \quad (1.12)$$

Since each chromophore oxy & de-oxy has specific extinction coefficient and DPF, measurement with two wavelengths leads to

$$\Delta OD = \begin{bmatrix}\Delta OD_{\lambda_1}\\ \Delta OD_{\lambda_2}\end{bmatrix} = \Delta C = \begin{bmatrix}\Delta C_{HbO}\\ \Delta C_{Hb}\end{bmatrix} \quad (1.13)$$

Eqn (1.13) provides a transformation of change in light output to relative change in concentration of chromophore. Thus, by knowing Extinction coefficient, path length and DPF, it is easy to compute relative change in chromophore concentration from change in attenuation. Since absolute concentration cannot be measured due to light scattering effects, all measurements are expressed as concentration changes from arbitrary baseline.

1.1.5 fNIRS Instrumentation:

NIRS instrument consists of a light source or emitting optode to deliver light into the tissues at a known intensity and at two or more wavelengths around the isobestic point and a detector or receiving optode to measure the intensity of exiting light. The receiver can be ipsilateral (Reflectance mode) or contralateral (Transmission mode)

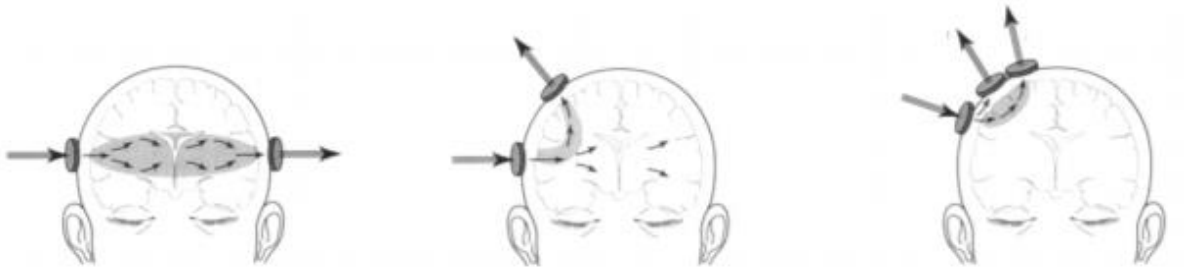

Transmission Mode Reflectance Mode Multi Distance

Figure 8: Types of fNIRs light transmission

(Source: https://www.researchgate.net/publication/224830755_Near-Infrared_Spectroscopy)

In transmission mode, there will be reduced intensity of the exiting near infrared light and hence signal-to-noise ratio will be poor. In reflectance mode, detector is placed ipsilateral to the source to minimize the loss of intensity which is sensitive enough for adults. In multi -distance approach, the light attenuation by skull and underlying tissues can be differentiated. There are diverse types of NIRS system based on the type of information needed.

1.1.5.1 CW-NIRS:

First type is continuous wave or CW NIRs which measures change in attenuation (ΔA or ΔOD) that can be linearly related to change in concentration of chromophore (ΔC) using Beer Lambert's law. It cannot measure absolute concentration due to loss of unknown amount of light in scattering and it is the most commonly used device.

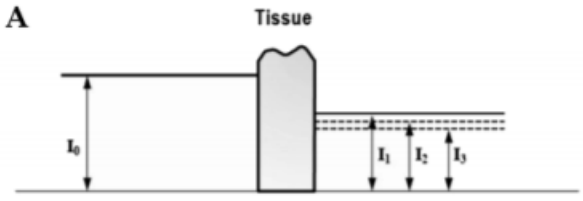

Figure 9: Continuous Wave NIRS

1.1.5.2 Time-Domain NIRs:

Second type is Time-domain NIRs which sends ultrashort pulses that propagated into the tissue and time of flight of photons can be detected. As a result of scattering, the time of photons coming out of the tissue has broader distribution called as Temporal Point Spread Function (TPSF) and concentration of chromophores can be obtained using the slope and extinction coefficient.

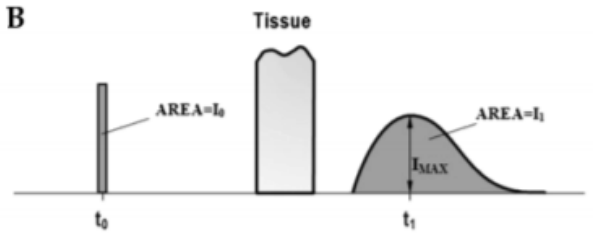

Figure 10: Time-domain NIRs

1.1.5.3 Frequency-domain NIRS:

Third type of NIRS instrument is frequency-domain NIRS which can measure attenuation, phase shift (Φ) & modulation depth of emerging light. For this present study, we have utilized CW fNIRS system.

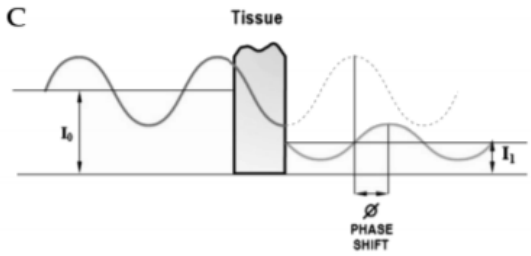

Figure 11: Frequency-domain NIRS

(Source: https://www.researchgate.net/publication/224830755_Near-Infrared_Spectroscopy[1])

Our fNIRs device utilizes frontal head probe with 4 LED modules or sources and 10 detectors. There are LEDs for each wavelength 730 nm and 850 nm (805 nm never activated). Each LED module are turned on for about 33ms sequentially (3). Therefore, in anyone of 500ms, there will be eight time slots of 33ms each, during which one LED at certain wavelength is turned on and the detectors are silicon avalanche photodiodes. Detector is placed at 2.5 cm away from the light source which collect photons that traveled along 'banana shaped path'. Photons interacted with tissue that travels banana path are the ones that have high probability of detection by each of the paired detector.

1.2 Physiology of Hemodynamic Response & Neuronal Activity:

Brain is the complex organ which requires adequate blood supply. Brain uses different mechanism called hyperemia to meet energy demands when local neurons are active (4). Neurons and astrocytes directly regulate local blood flow within capillaries resulting in neurovascular coupling. Metabolic signals like decrease in O_2 or glucose concentration or excess CO_2 causes local increase in blood flow upon neuronal firing.

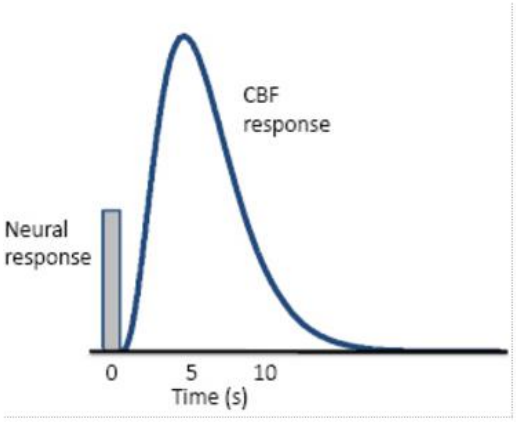

Figure 12: Hemodynamic Response Function

(Source: http://journal.frontiersin.org/article/10.3389/fnene.2010.00025/full)

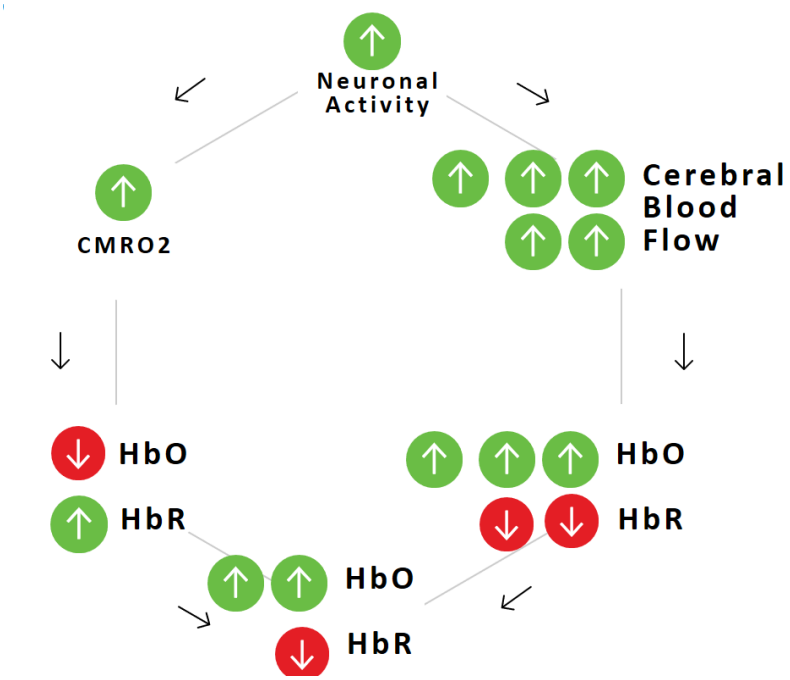

Figure 13: Neurovascular Coupling

(Source: http://journal.frontiersin.org/article/10.3389/fnene.2010.00025/full)

Fig (13) represent neurovascular coupling i.e. how neuronal activity is correlated to cerebral blood flow. Neural activation in response to a stimulus results in increased energy demands near the area of brain activated. To accommodate this energy demand, cerebral blood flow (CBF) increases to the activated brain areas carrying more O_2 and glucose due to vasodilation. This change in blood flow is accompanied by increase in blood volume and can be measured by local change in concentration of oxy-hemoglobin (HbO) and de-oxyhemoglobin (Hb). (Source: https://users.fmrib.ox.ac.uk/~stuart/thesis/chapter_3/section3_3.html)

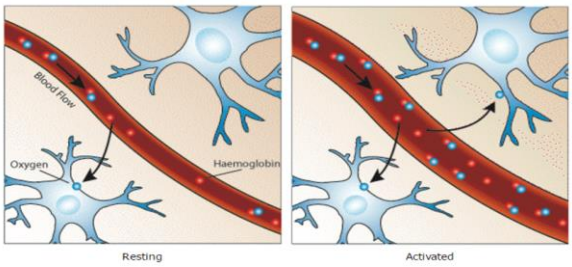

Figure 14: Resting & Activated Cerebral Blood flow

Generally, during cortical activation, local concentration of oxy-hemoglobin (HbO) increase, whereas concentration of de-oxy hemoglobin (Hb) decrease. As CBF and cerebral blood volume (CBV) increases, there is an increase in O_2 availability to produce more ATP to supply neurons with more energy. To capitalize on these hemodynamic changes, fNIRs is used to measure light intensity at stimulus duration and comparing it to light intensity during baseline (4) event when there is no stimulus presentation. Under various pathological conditions which disrupts neurovascular coupling, there will be alterations in regional blood supply at the cerebral level to meet local energy demands. Thus, fNIRs can serve as a good functional neuroimaging technique providing results that are consistent with fMRI /PET as there exists linear relationship between hemodynamics and neural activity.

1.3 Neurophysiology of Prefrontal cortex (PFC):

In the light of the experiment described in chapter 2, it is in the prefrontal cortex that we are looking for changes in neuron activity and underlying hemodynamics for certain tasks. Prefrontal cortex is the region of cerebral cortex often called as multi-modal association cortex (5) as the processed information from various sensory modalities are integrated here in a precise manner to form physiological constructs of working memory, perception and many other cognitive processes. Many 'executive' functions and their localizations are associated with specific regions of PFC. Frontal lobe is mainly occupied by the PFC on its medial, lateral and orbital surfaces and it is the region that undergo full myelination during adolescence. It constitutes major feed-forward and feedback circuits for information processing in brain. It includes Brodmann areas BA8,BA9,BA10,BA11,BA12,BA13,BA14,BA24,BA25,BA32,BA44,BA45, BA46 & BA47(5). Lateral PFC is associated with language, attention, memory ,novelty processing required for new learning, creativity, explicit memory, memory encoding & retrieving. Right Dorso lateral Prefrontal Cortex (DLPFC) mediates negative attitudes and left ventrolateral prefrontal cortex (VLPFC) is associated with positive attitude, planning etc. Many researches have shown that Medial

PFC is associated with attention to demanding cognitive task, spatial memory, perception of pain in coordination with anterior cingulate cortex, Reward and goal-directed activity. Orbitofrontal regions are involved in response inhibition, processing of outcomes even if there is no reward, emotional processing and delayed response.

This study was conducted to characterize and monitor hemodynamic changes in PFC associated with certain neurocognitive tasks related to response inhibition, sustained attention and semantic perception for healthy subjects and also to study chemobrain.

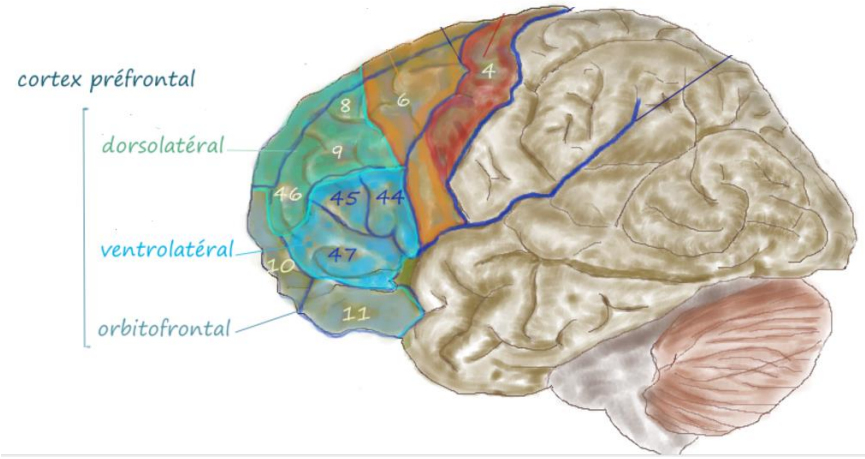

Figure 15: Functional Organization of PFC

(Source: https://en.wikipedia.org/wiki/Dorsolateral_prefrontal_cortex)

1.4 Cancer Related Neuro Cognitive Dysfunction (CRND) or Chemo brain

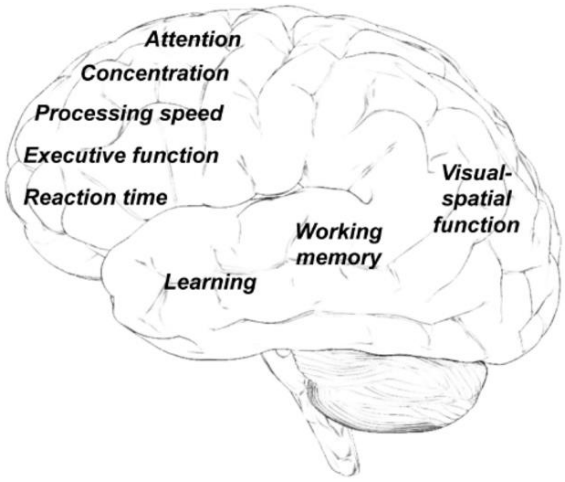

Figure 16: Clinical Characteristics -Chemo brain

(Source: http://www.ascopost.com/issues/october-15-2012/cognitive-impairment-in-patients-with-cancer/)

In recent years, there has been growing evidence to support an increased incidence of cancer and related cognitive decline in cancer survivors due to chemotherapy. (6) Chemotherapy refers to the cancer treatment that utilizes certain drugs/chemicals to treat cancer patients. Chemotherapeutic drugs mainly aimed at preventing cancer cells from proliferation and its invasion to neighboring tissues. Because cell proliferation is a common characteristic of any normal cell, these chemotherapeutic agents are found to have toxic effect normal cells which leads to neurological toxicity and other side effects that damages Central Nervous System (CNS). According to researchers (7), many cancer survivors experience cognitive decline while undergoing chemotherapy and in some patients, changes persist for years even after treatment which seriously affect their quality of life. Among many unpleasant side effects of cancer and chemotherapy, cognitive impairment is the biggest challenge for patients. Commonly called

as chemo brain or chemofog, the problems with working memory, multi-tasking, decision making, concentration, reasoning, visuospatial skills sometimes even speech have devastating effect on patients' lives. Overall nature of chemotherapy induced cognitive impairment cannot be defined exactly because of the presence of several pathogenic mechanisms by which chemotherapy may impact cognitive ability. Neuroimaging tools such as fNIRs provide unique means for assessing brains structural changes or neuronal activity & cognitive behavioral results which would provide practical solutions for chemobrain related research questions that can improve the quality of cancer survivors.

1.4.1 Chemo brain

Chemo brain is the term used to describe the alterations in cognitive functioning due to CNS toxic effects of chemotherapy. Based on one's susceptibility, genetic factors that regulated neurotransmission, Blood brain barrier transporters may increase the vulnerability of an individual to cognitive changes due to chemotherapy. Research studies suggest that chemotherapy can cause cell death and reduce cell division of not only proliferating cancer cells but also normal cells which are crucial for cognition. Chemotherapy may also lead to poor deoxy ribonucleic acid (DNA) repair mechanisms. Patients undergoing chemotherapy tend to have high degree of fatigue as a side-effect of treatment. They also suffer from depression, anxiety, and other mood disorders which have negative effect on cognitive function.

Previous studies using neuroimaging studies to assess chemotherapy related changes in brain structures, functions and behavioral performance on breast cancer patients indicated significant changes in frontal, parietal, and occipital white matter and deficits in attention, psychomotor speed, reaction time and memory . There is also an evidence of changes in blood flow to key regions in brain mainly in pre-frontal cortex, parietal regions and cerebellum for the breast cancer patients treated with chemotherapy .

fNIRs can be a better neuroimaging tool to validate these neuropsychological measures in cancer population which could facilitate the assessment and evaluation of intervention to extenuate CRND.

1.4.2 Mechanisms of CRND:

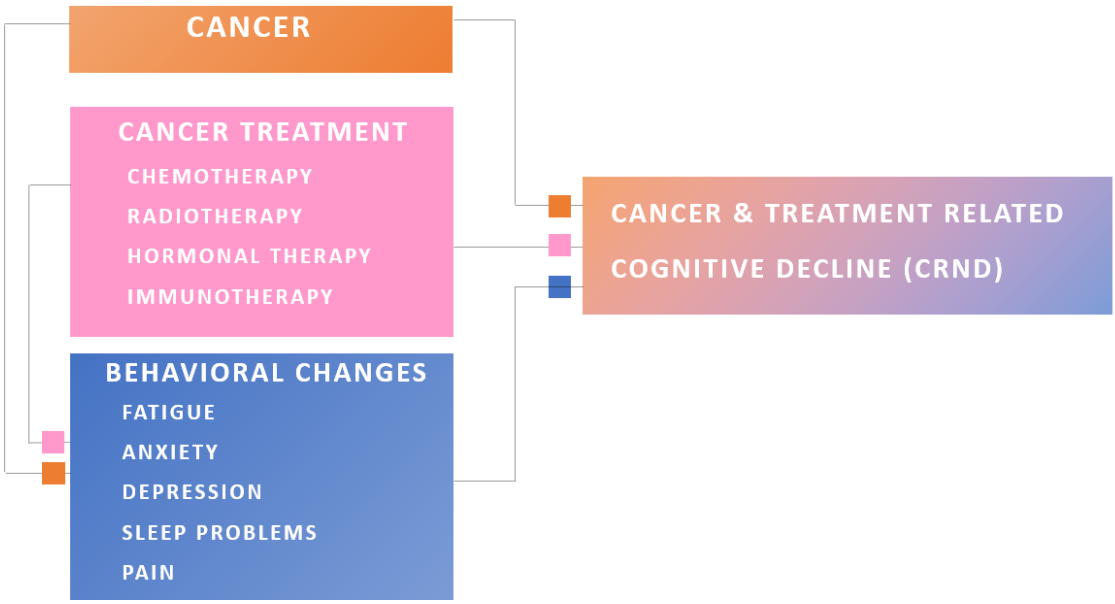

Figure 17: Causes for CRND

(Source: Jean-Pierre 408-414) NeuroImage 85 (2014): 408-414)

CRND may be either caused by chemotherapy as a treatment of cancer or by cancer itself. Although several mechanisms such as neurotoxic injury, decreased neurogenesis, hormonal pathway and neuroinflammation have been proposed, the exact underlying mechanism by which chemotherapy or cancer brings about the structural or functional changes in brain is still a matter of debate (1,3). As most of the drugs will not be able to cross Blood Brain Barrier (BBB) that cause direct damage to brain cells, the cognitive effects are thought to be probably a secondary result of systemic inflammation caused by chemotherapy. Or Chemotherapy drugs may develop genetic alterations in transporters of BBB thus

allowing small amount of drug to enter brain. These drugs also cause damage to CNS progenitor cells and oligodendrocytes which eventually leads to myelin damage. Hormonal changes secondary to chemotherapy induced menopause can also affect cognition on patients because of decreased levels in estrogen hormones that are neuroprotective. Another potential mechanism of CICI is DNA damage which affects CNS secondary to increased oxidative stress (2). Oxidative stress is mainly caused as a result of production of reactive oxygen species which includes free radicals & peroxides that cause DNA damage.

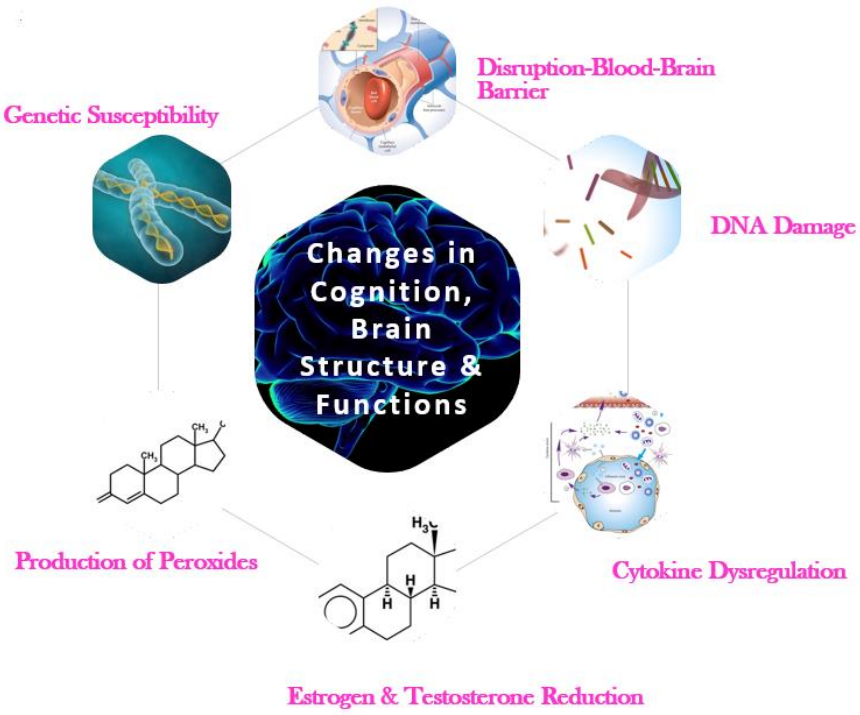

Figure 18: Mechanisms of CRND

(Source: http://www.sciencedirect.com/science/article/pii/S0749208113000545)

Cancer related anemia is another side effect of cancer itself which is capable of inducing cognitive and visual memory impairment, decreased executive function tasks because of poor cerebral oxygenation Mostly patients develop long term side effects because of chemotherapeutic drugs. Finally, pathogenesis

of CRND may also be attributed to immune dysregulation with the release of inflammatory cytokines and is mainly seen in patients treated with immunotherapies. These patients tend to exhibit higher cytokine levels due to neuroinflammation which is associated with cognitive disruption including poor executive functions and reaction time. There is no way to prevent CRND but the focus is to improve the quality of life of affected survivors during and after treatment by knowing the metabolic and behavioral changes.

1.4.3 Clinical characteristics of CRND:

Main Cognitive skills that are affected due to CRND includes memory, executive function, processing speed , concentration & reaction time abilities. Sometimes, CRND persist for a long time even after the discontinuation of chemotherapy. The affected cognitive tasks and the brain areas involved are shown in figure (19). Mainly the emotional distress caused due to cancer diagnosis or administration of chemotherapeutic drugs are the strong reasons for psychosomatic variations in cancer survivors. Once emotional distress appears in cancer patients it is long-term even after the completion of treatment. Main symptoms for CRND includes memory lapses-difficulty in recalling, trouble concentrating or finishing tasks, difficult in remembering details and familiar words, less attention, feeling foggy.

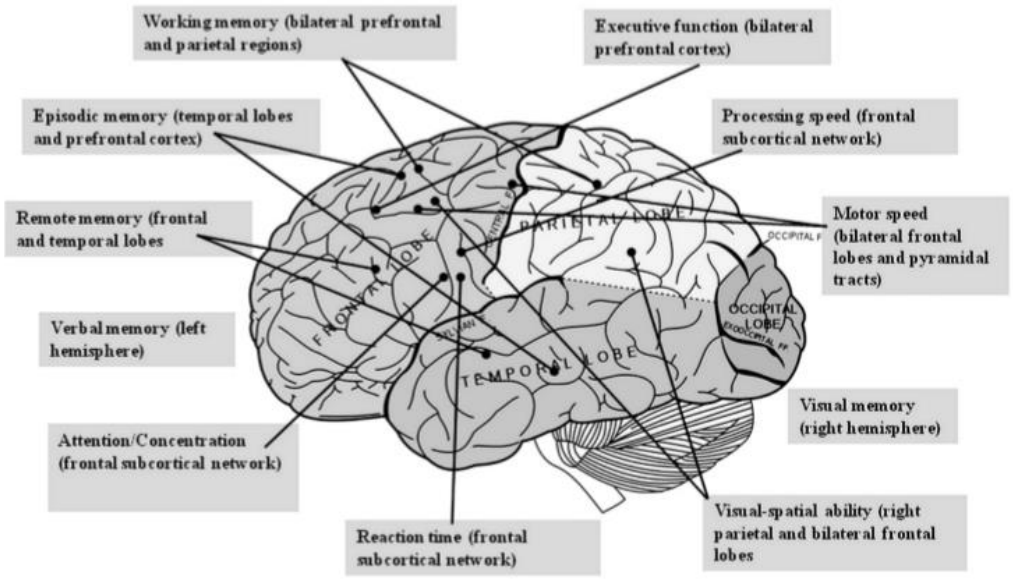

Figure 19: Symptoms of Chemo brain

(Source: Argyriou, Assimakopoulos, Iconomou, Giannakopoulou, & Kalofonos, 2011)

Two other main mechanisms or clinical changes are reported by many researchers even though they have not been studied with chemotherapy related cognitive changes. First mechanism is that many chemotherapeutic drugs are cardiotoxic. i.e. they cause cardiovascular changes. And these cognitive changes could possibly be secondary effect to cardiovascular variations that could influence cerebral changes. Second is that neuroendocrine changes due to chemotherapy could alter neurocognition (3).Many cognitive tests and experimental paradigms using different neuroimaging tools like fNIRS can be used to evaluate neuronal activities and to understand complete mechanisms behind this cognitive decline which would help patients to improve their quality of life.

1.5 Focus of this study:

Many useful neuroimaging tools such as fMRI, SPECT, PET,CT and others are available to map cognitive functions to brain structures and to successfully describe the effects of cancer. But they can be very expensive and it makes impractical to use those imaging tools to screen Chemotherapy related

cognitive impairments. Although fMRI is the current 'gold standard' in functional imaging research, this method is restrictive in that it is loud, expensive and susceptible to movement artifacts and it requires patient to be exposed to magnetic field and radioactive traces. But fNIRs is less expensive, safe and non-invasive and best suited for screening and assessment of CRND.

The primary goal of this study is to investigate the feasibility of using functional near infrared spectroscopy (fNIRs) to monitor hemodynamic changes in prefrontal cortex induced by certain neuropsychological tests in healthy young and older subjects and also to compare it with cancer survivors to identify possible functional biomarker. Functional brain imaging using fNIRs has been used in neuroscience to examine cortical activities and performance of visual, motor ,cognitive tasks in many healthy and diseased populations with attention deficits, depression etc. Previous studies have utilized neuroimaging techniques such as DTI, fMRI, PET to assess treatment related changes in neurocognitive performance, brain structural alterations. Deprez et al used Diffuse Tensor Imaging (DTI) to study the effects of chemotherapy on white matter in brain and cognitive performance in premenopausal women with breast cancer. They found significant structural changes in fronto-parietal regions and decrease in memory and processing speed.

In this study, we aimed at examining the hemodynamic changes in frontal region of brain due to cancer and related treatment to get to know the affected areas and treat this condition. For now, we are examining the feasibility of monitoring HbO changes triggered by certain neuropsychological stimuli using fNIRS on healthy subjects which could be applied to cancer patients before, during and after treatment. This could help us better understand if the cognitive disability is due to chemotherapy or the cancer itself. Statistical and hemodynamic results are presented to understand neural activation patterns and observed the prefrontal activity in response to certain stimuli in healthy subjects.

1.6 Outline of this study

Chapter 1 consists of brief introduction about fNIRs, physiology of PFC and hemodynamic response & Chemobrain. Chapter 2 is about the investigation of hemodynamic response in PFC using fNIRs, subjects under consideration, experimental protocol, cognitive tasks involved, instrumentation & data analysis methods used. The hemodynamic and statistical results to assess behavioral and hemodynamic measures are presented in chapter 3. Chapter 4 explains about the result obtained, discussions, physiology behind the results, limitations of this study & future direction of this work.

Chapter -2

Methodology

This section describes the experimental methodology and protocols used for this study. The data were collected from a group at University of Notre Dame. The healthy subjects were divided into two subgroups based on age group namely young & older adults. Subject who fall under the age of 18-25 were categorized as young adults and those who are in their 40-75 are grouped as older adults. They were asked to perform few cognitive tests namely N-back (working memory task), Go/No-Go (Sustained attention and response inhibition) & Stroop (Cognitive interference) and their blood flow changes were measured. Hemodynamic responses were compared between younger & older adults.

2.1 Selection of Subjects:

Figure 20: Demographics in this study

The protocols & experimental procedures used in this study was reviewed and approved by the Institutional Review Board of Florida State University School of Medicine and compliant with NIH guidelines. Healthy young and older adults of either genders who met the eligibility criteria were recruited for this study. Younger adults (9-younger adults) of age group between 18-25 and older adults (6-older adults) of age group between 40-75 from any race and ethnicity were taken into consideration. A total of 15 participants were enrolled for this study. Eligible participants were asked to sign in the

consent form after explanation of study's purpose, experimental procedure, possible risks & benefits and they were asked to fill out questionnaire about the history of smoking, alcohol, intake of any medication, or any other illness. Participant's demographics such as gender, age, marital status, handedness was also noted.

Few behavioral scores such as Hamilton Anxiety & Depression scale (HADS), Cognitive Failure questionnaire (CFQ), Insomnia Severity Index for sleep (ISI), Need for cognition scale (NCS), Fatigue severity scale were recorded. Before the start of every experiment, a signed consent form was obtained.

2.2 Instrumentation

2.2.1 fNIRs system:

fNIRs system is a portable optical functional neuroimaging tool capable of monitoring the brain hemodynamics when performing certain cognitive or motor tasks in naturalistic way. NIRS measurements were performed using a continuous wave (CW) multi-channel NIRS system BIOPAC fNIRs 100A (BIOPAC Systems Inc., Santa Barbara, CA, USA) that includes Cognitive Optical Brain Imaging (COBI) Studio Software (fNIR Devices, Potomac, MD, USA). This fNIRs system utilizes two wavelengths 730 nm & 850 nm of continuous near-infrared light.

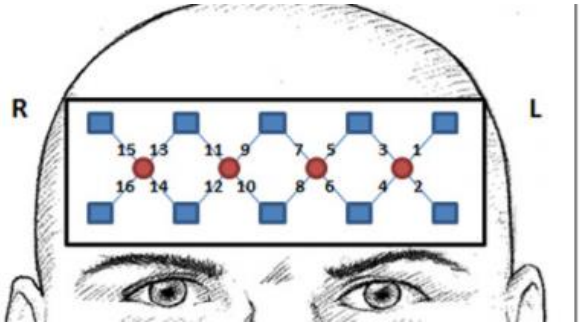

Figure 21: Location of optodes on PFC

(Source: Biopac fNIRs)

There was a total of 14 optodes consisting of 4 LED light sources with an inter-optode distance of 2.5 cm and 10 photo detectors made of silicon photodiode arranged in a pattern covering the prefrontal cortex (Figure 21) that enabled the measurable cortical activation over 16 channels (Channels 1-8 -left hemisphere; channels 9-16- right hemisphere).One source and one detector forms single channel. Each light source has 2 LEDs with wavelengths of 730nm and 850 nm to differentiate absorption spectra of de-oxy and oxy chromophores respectively. System has temporal resolution of 500ms for one complete data acquisition cycle. This fNIRs device records hemodynamics at a frequency of 1.9608 Hz and consists of a sensor pad of 180 X 60 X 8mm.

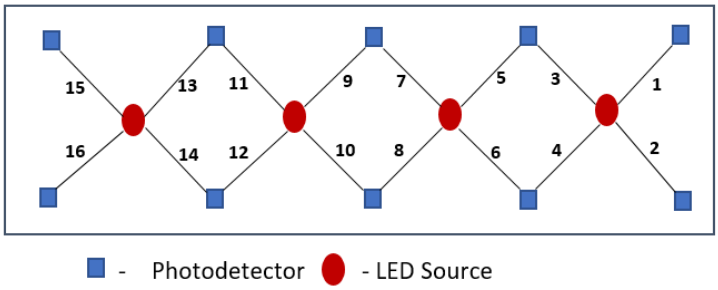

Figure 22: Arrangement of Sources and detectors

fNIRs sensor detects the concentration of HbO and Hb in real-time during various stimuli. The COBI studio data collection software allows us to monitor PFC hemodynamic response in real time and to present participants with certain cognitive tasks. 16-Channel Probe was placed on the forehead 0.5 cm above eyebrow aligned to Fp1 and Fp2 of international 10-20 system with Fpz as the midpoint of the probe . Care was taken to avoid hair from interfering with detectors and sources.

2.3 Protocol / Experimental Paradigm

2.3.1 N-back Task:

N-back test provides varying task-load conditions to test associations between level of difficulty and cortical activation. A blocked periodic design that incorporated alternating 0-back,1-back, 2-back,3-back tasks was used during Working Memory Task. There were three blocks in each back condition and so there were a total of 12-blocks with baseline period of 120s. Within each block, many letters were pseudo randomly shown to the participants. Participants must continuously remember the last n of a series of rapidly flashing letters. It requires subjects to react when a stimulus is the same as the n-th letter before the stimulus letter. We denote a letter stimulus, which is same as the one n previously as target. Subjects had to press 'Yes' or 'No' when the letter is shown on gray screen when they encountered a target.

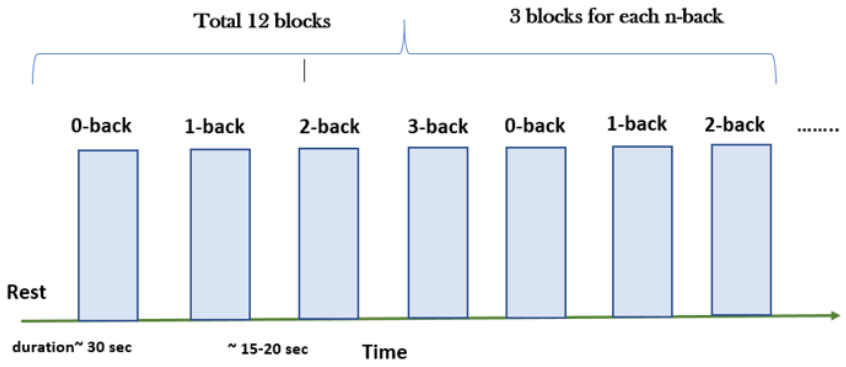

Figure 23: Experimental Paradigm-N-back

With increasing 'n', the task difficulty increases, as the subjects have to remember more letters and continuously shift the remembered sequence. Sometimes, we can also measure performance in this task by measuring the amount of missed targets (when the subjects do not press the key for a target) and through the amount of wrong reactions (when subjects incorrectly identify stimulus as target). A total of

25 letters was presented during every block with each letter for 500ms resulting in trial length of around 30 sec followed by inter block interval of around 15-20s. In 1-back test, participants were instructed to respond if the stimulus was same as in the previous trial (9). In 2-back test, participants were instructed respond if the stimulus was same as in two trials previously and for 3-back it is three trials previously. Epochs were presented in the order Rest-0B-1B-2B-3B-0B-1B-2B-3B-0B-1B-2B-3B. To ensure each participant understood the instructions correctly, they were asked to practice all blocks before the experiment. Figure (23) shows experimental protocol. The order of different n-back conditions was in the increasing order from 0-back to 3-back and fNIRs data was recorded continuously during the entire session.

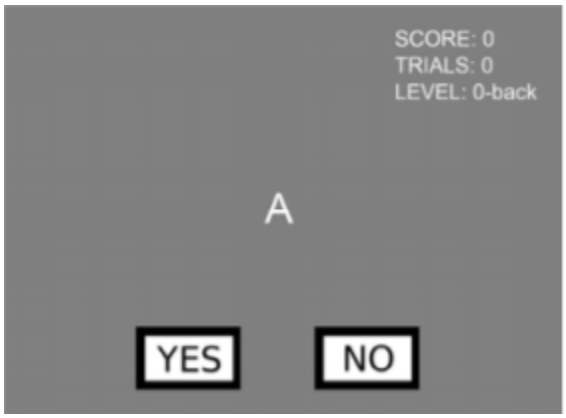

Figure 24: Screen for 0-back

(Source: https://scholarblogs.emory.edu/nbbparis/files/2015/06/10.1371-journal.pone_.0099222.g001.png)

2.3.2 Go/No-Go Task:

We investigated inhibition-related hemodynamic activation when subjects performed go/no-go task. We examined it for both older adults and younger adults. This task consisted of Baseline of 120 s, go (G) and no-go (NG) epochs in pseudo randomized order starting from Rest with Total of 8 blocks consisting of four blocks of Go and four blocks of No-Go . During Rest epoch, participants passively viewed a

blank screen with each task block lasted for 30 seconds and interstimulus interval was 500 ms. A total of 25 letters was presented during every block and there is an inter block distance of around 20 s. During 'Go' epochs, participants were instructed to press a button with their index finger each time a letter appeared on the screen. During No-Go epochs, participants were instructed to push a button for all letters except X. And for X, they should withhold their response. Figure (25) explains the experimental protocol.

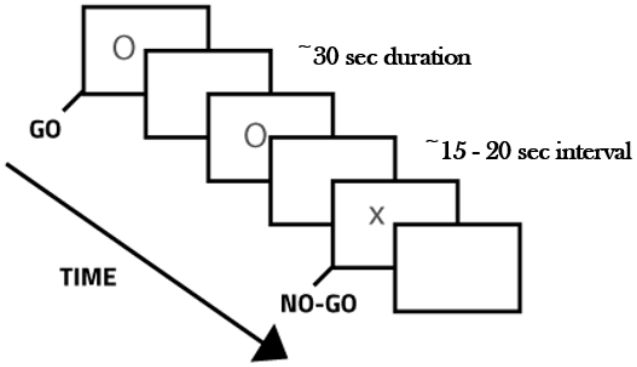

Figure 25: Experimental protocol-Go/No-Go

Figure 26: Block Diagram- Go/No-Go

2.3.3 Stroop Task:

In this task, subjects were required to focus on the center of the screen guided by fixation object '+' followed by stimuli. Participants were presented with Neutral, Congruent and Incongruent stimuli on a black background.

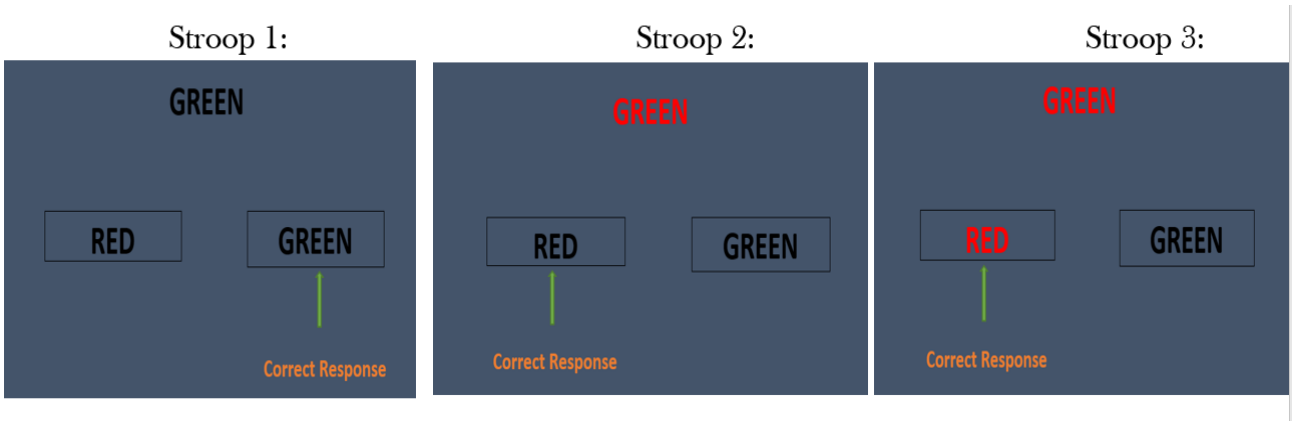

Figure 27: Stroop Task

The stroop task was divided into three namely stroop1 which was neutral, stroop2 which was congruent and stroop3 which was incongruent. Each stroop had total 3 blocks with 25 presentations and started with a baseline of 120 seconds. The duration of each block was varying between 30-50 seconds and interblock interval was around 20 seconds. The stroop color word task consisted of Red, Green and blue colored square boxes with corresponding written words. The duration of each presented square box was 500ms each. For stroop 1-neutral trials, squared color boxes were shown, followed by words written in white. For Stroop 2- Congruent trials, squared boxes with words describing the color of the box written in same color (ex. RED color box with printed word RED in RED ink) were presented to the participants. For stroop 3- Incongruent trials, squared boxes with words written in a color other than color of the box (ex. BLUE color box with printed word BLUE written in RED color ink). Subjects were asked to reply quickly and accurately to name the color word while ignoring the color itself (color of the box) with a button press.

2.4 Data Analysis:

2.4.1 Data Screening & Pre-processing:

Using Modified Beer-Lamberts law, changes in concentration of oxygenated hemoglobin (HbO) relative to initial resting baseline (which sets the activation level to zero) prior to each condition response extracted from raw fNIR data (16 channels X 2 wavelengths). HbO concentration change was measured relative to the baseline (zero) in micro molar units (μM). Raw HbO data was collected using COBI software and were preprocessed and analysed using MATLAB (The MathWorks Inc., Natick, MA, 2000). All recorded fNIR signals were first low-pass filtered, with cut-off frequency of 0.2 Hz and high-pass filtered with cut-off frequency of 0.01 Hz to remove slow drifts. Low-pass filtering removes a lot of cardiac pulsation signal centered around 1 Hz. However, other sources of hemodynamic oxygenation fluctuations such as breathing and Meyer waves overlap in frequency with relevant activation signal frequencies. To remove these physiological fluctuations, we exploited the fact that those systemic signals are global in nature and therefore appear in all measurement channels. Global signals were regressed out by taking the average of the signal across all channels within the measured brain region from channel-wise data .This signal averaging mainly regress out the common global systemic frequency fluctuations which may be the artifacts including head movements. Measured and filtered data were subjected to standard analysis procedure using General Linear Model, GLM.

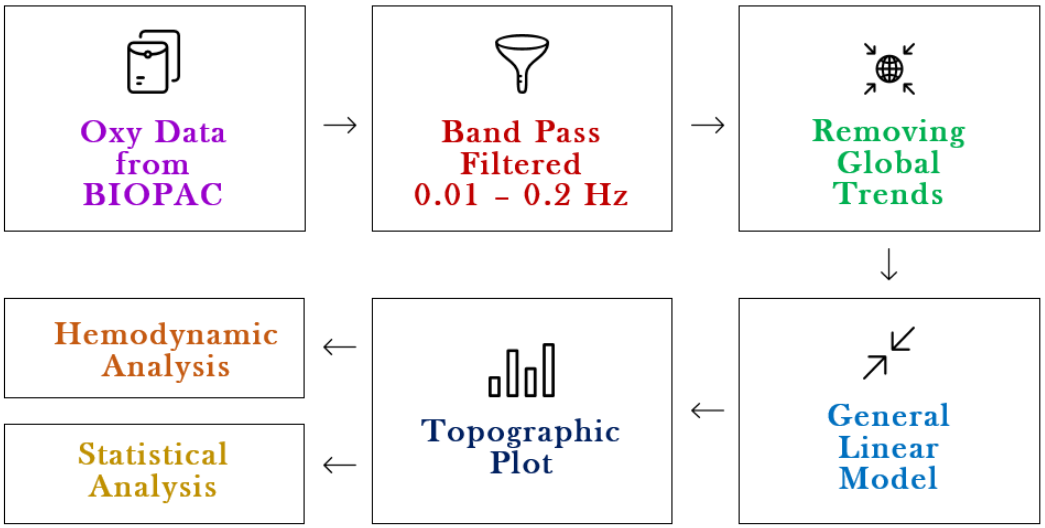

Figure 28: Data processing overall Flow

2.4.2 General Linear Model

In the standard General Linear Model (GLM), the contributions of individual hemodynamic changes for each block are summed and assumption of linearity generally holds true as inter stimulus interval is sufficiently long (> 4-6 seconds) for all the tasks (Abdelnour & Huppert, 2009). This general linear model extracts the activation response from each fNIRs channel by convolving a boxcar function (representing a stimulus) reflecting the activation interval with a canonical hemodynamic response function (HRF) or a gamma function. GLM model was given by,

$$Y = X\beta + \epsilon$$

where X denotes the design matrices or stimulus and β is the corresponding response signal strength for oxy-Hb or de-oxy Hb and Y represents the original fNIRs time series output (with dimensions: Number of Time points X Channels). Hemodynamic response function was used to model Blood Oxygen Level Dependent (BOLD) signal in response to neuronal activity. Each channel was analyzed using GLM with regression to the following HRF. HRF is represented by a typical gamma function which can be

covolved with Predictor/Regressor. For example, in n-back, each of the back conditions and its onset & duration forms each regressor. Since we had four n-back conditions, we took four regressors.

The activation amplitude represented by changes in HbO and HbR, relative to the baseline in each channel and they were extracted from the regression fit. β-values/ weights(Activation amplitude changes) which are found from General Linear Model for each individual subject were grouped for younger adults and older adults and for each task.

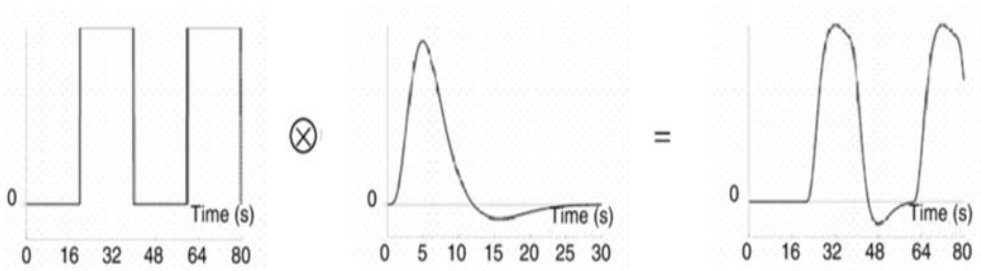

Figure 29: General Linear Model- Regressor

(Source: http://www.brainvoyager.com/bvqx/doc/UsersGuide/StatisticalAnalysis/TheGeneralLinearModel.html)

2.4.3 Topographical plots:

These β-values for younger and older adults were plotted as topographical plots by utilizing spline interpolation. Our intention was to map hemodynamic response onto a topographic plot by choosing linear methods of interpolation. The channel positions were used to define grid points for accuracy of topographic maps. All grid points were assumed to be square of equal area consisting of 8 X 2 map elements to describe the location of channels. And the beta responses calculated from General linear model were interpolated to neighborhood pixels of grid element.

2.4.4 Statistical Analysis:

Statistical Analysis is little complicated here as multiple measurements were taken per subject. That is, each subject has provided multiple responses which would violate the assumption of independence. So, analysis was carried out in two ways. One approach for statistical analysis was to fit the data to a linear mixed effect model and other approach was to perform two-sample t-test between cancer & healthy older adults and to compare Healthy Young Vs older adults.

2.4.4.1 Linear Mixed Effect Model:

Multiple responses from single subject cannot be regarded as different from each other. Every person has slightly different response for various tasks and this is going to be an idiosyncratic factor that affects all responses from same subject which leads to an idea that these different responses are inter-dependent. This situation was dealt by adding a random effect for subjects. This non-independence was resolved by assuming different baseline factor for each subject. This was done by assuming random intercepts for each subject. Thus, a random effect was added for 'Subject' and this has resolved the problem caused due to individual differences.

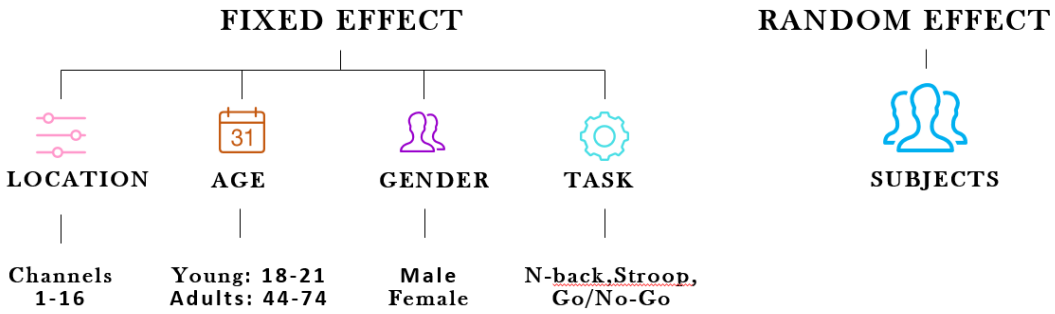

Figure 30: Linear Mixed Effect Model

The focus was studying the effect of location (channel), age, gender and task on the response variable 'β' or the regressions coefficients which represent the activation amplitude denoting the concentration changes in HbO relative to baseline in each channel. Location, age , gender, and task were considered to be fixed main effects while subject was taken as random effect since repeated measurements were taken. Since, there is combination of fixed and random effect, this model is considered to be linear mixed effect model. We had 16 channels or locations and location 1 was considered as baseline and other location were compared to with respect to channel 1.

2.4.4.2 Two Sample t-tests:

Two sample t-tests were performed to identify if responses for cancer and healthy older adults were significantly different and also to identify which location has shown the difference. The t-tests were performed between beta responses for each channel from 3 cancer survivors and 6 healthy old adults and they were tested under 95% confidence interval. The null hypothesis of this test was that the responses of cancer patients were not statistically different from healthy adults in each of the selected channel. This t-test was carried out channel-wise for cancer and healthy controls. This test was done for all selected 16 channels and for all the task paradigms.

Another two-tailed, two sample t-test was performed to evaluate if the channel responses for healthy old and young adults were statistically different. The t-tests were performed channel-wise and for each of the channels between healthy older adults and healthy younger adults. This was performed to identify the channel which has shown significant difference between older and younger adults and the data where tested under 95% confidence.

Chapter-3

Results

This section has detailed the experimental results obtained from the analysis carried out based on the processing methods mentioned in the previous section.

Table 1: Demographics of Younger Adults (18-21)

S No	Patient ID	Age	Gender
1	3	18	Female
2	4	21	Female
3	10	20	Female
4	11	20	Female
5	12	21	Female
6	13	20	Female
7	15	18	Male
8	16	19	Male
9	17	21	Female
10	21	19	Female

Table 2: Demographics of Older Adults (44-74)

S No	Patient ID	Age	Gender

1	14	44	Male
2	18	48	Male
3	19	74	Female
4	20	59	Female
5	22	54	Female
6	23	72	Female

Table 3: Demographics of Cancer Patients (38-59)

S No	Patient ID	Age	Gender
1	3	59	Female
2	4	38	Female
3	5	43	Female

3.1. Hemodynamic Responses

Hemodynamic Response analysis was done using GLM. Beta values were obtained for HbO and Hb concentrations but for this study, only HbO concentration changes were analyzed. These beta values were plotted as images that showed task evoked activation response in prefrontal cortex under various neuropsychological tests. The obtained images were generated using MATLAB and statistical test was carried out to evaluate if the response locations were statistically different.

3.1.1. Hemodynamic Response: N-back Test

The below figure (31) showed hemodynamic response of pre-frontal cortex for n-back test which consisted of 12 blocks in total with 3 blocks for each of the n-back condition. The responses were measured for 120s baseline period and during 30-40s verbal n-back task.

3.1.1.1 Healthy Old Vs Healthy Young 0-back

Old

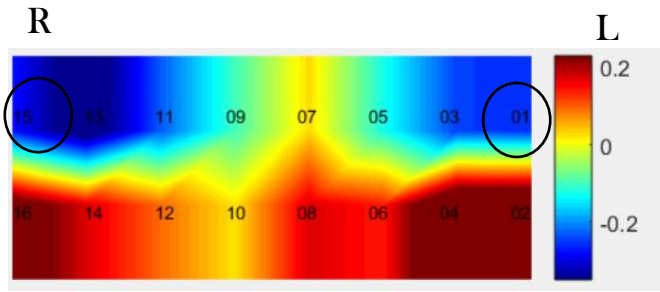

Young

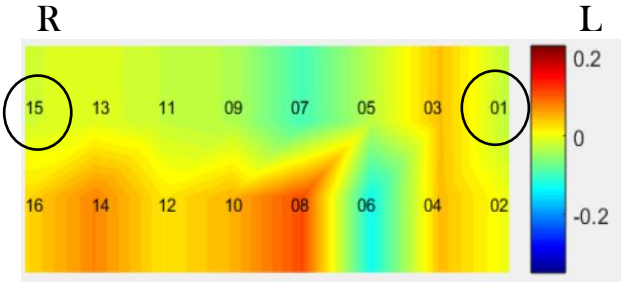

1-back

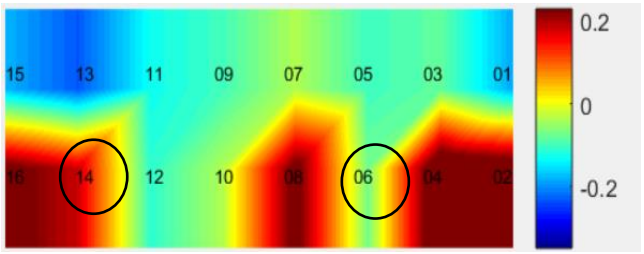

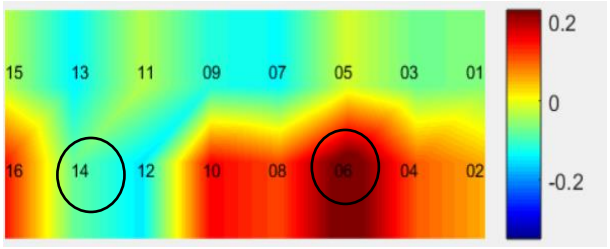

2-back

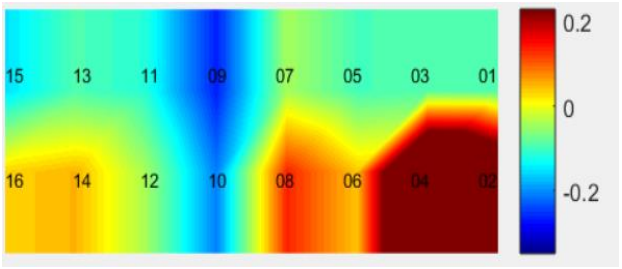

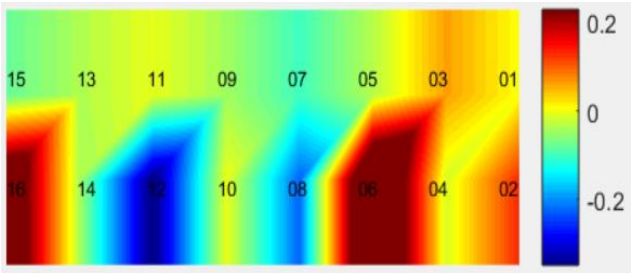

3-back

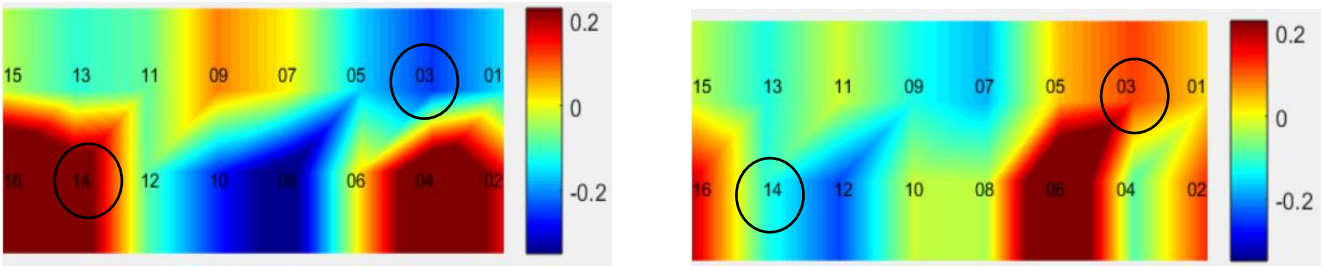

Figure 31: Young Vs Old: Hemodynamic Response of n-back

Figure (31) shows hemodynamic response comparison between healthy young & healthy old adults. Encircled channels are found to be significantly different after doing two-sample t-test between Healthy Old Vs young as well as Cancer vs healthy old. For example, channel 1, 15 are significantly different for 0-back condition between old vs young. Channel 6 & 14 for 1-back, Channel 3 & 14 for 3-back were found to show significance. Also, if we observe, there is no lateralization effect seen in older adults and only bilateral activation was seen. But Right-hemispheric dominance is seen in younger adults for 0-back but they started recruiting left hemisphere as the memory-load increases. In young adults, left pre-frontal activation was observed with increasing memory load.

3.1.1.2 Cancer Vs Healthy old

The below figure showed hemodynamic response of pre-frontal cortex for n-back test between cancer & healthy adults. The responses were measured for 120s baseline period and during 30-40s verbal n-back task.

0-back

Healthy Old

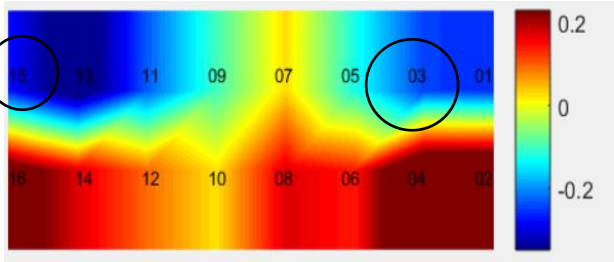

Cancer

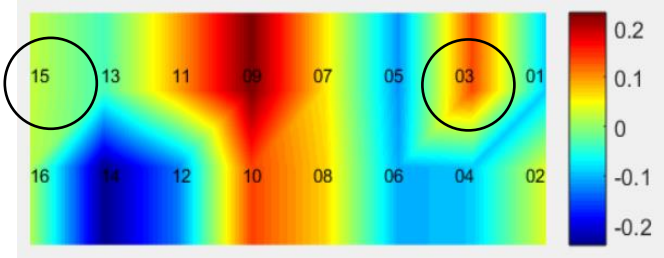

1-back

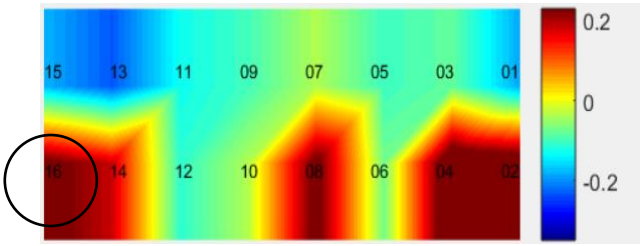

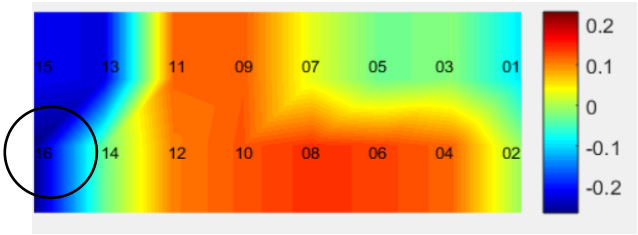

2-back

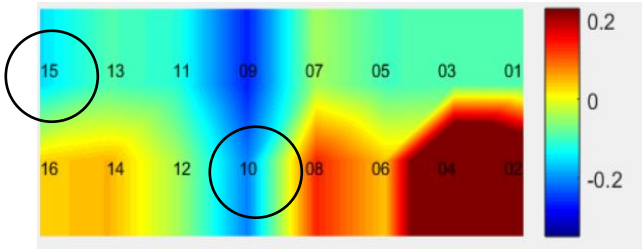

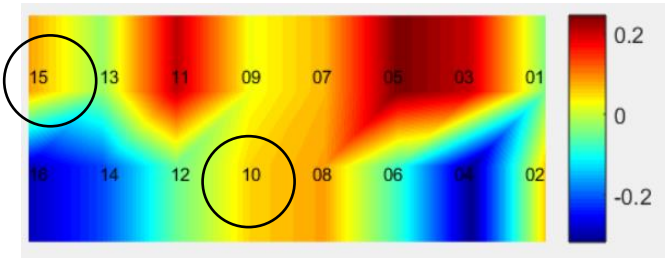

3-back

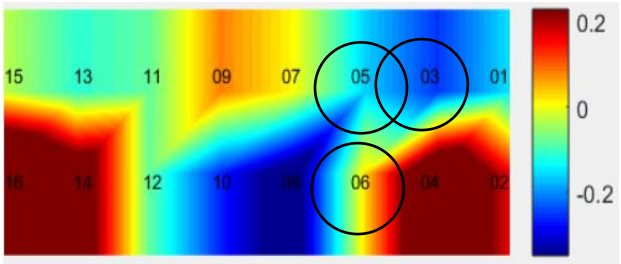

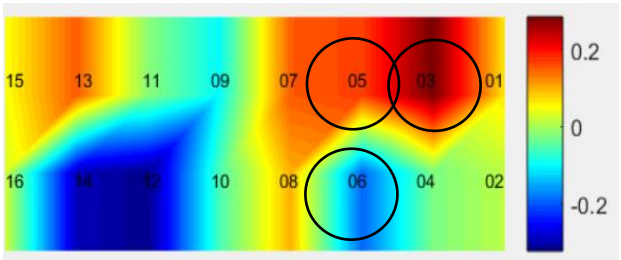

Figure 32: Cancer Vs Healthy: Hemodynamic Response of N-back

Figure (32) shows hemodynamic response comparison between cancer & healthy adults. Circled channels are found to be significantly different between cancer & healthy individuals. For example, in 0-back condition, Channel 3 and 15 lying in DLPFC were showing difference, for 1-back, Channel 16, for 2-back, channel 10 in MFC and channel 15 in DLPFC, for 3-back, channel 3, 15 & 6 were identified to shown some difference. And we also observed bilateral activation for healthy subjects but there is deactivation in right VLPFC for all the N-back conditions and significant activation in DLPFC for cancer patients.

3.1.2. Hemodynamic Response: Go/No-Go Test

The below figure (33) showed hemodynamic response of pre-frontal cortex for attention-inhibition task between healthy older & young adults. The responses were measured for 120s baseline period and during 30-40s go/no-go stimuli with inter-block interval of 15-20 sec.

3.1.2.1 Healthy Old Vs Healthy Young

Old Young

Go Condition

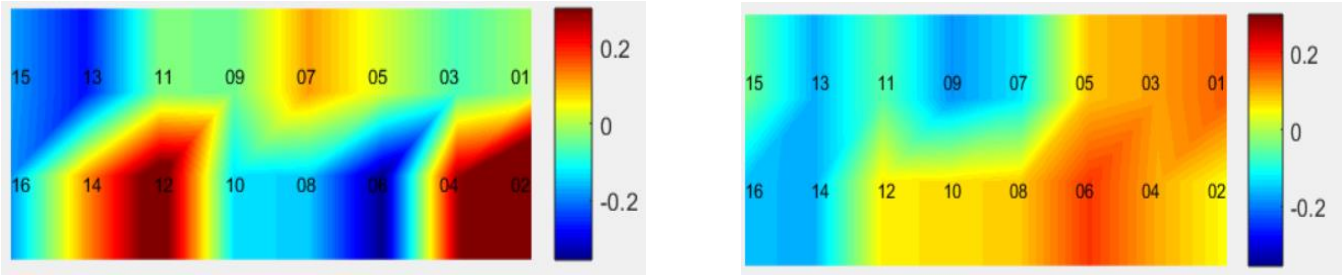

No-go Condition

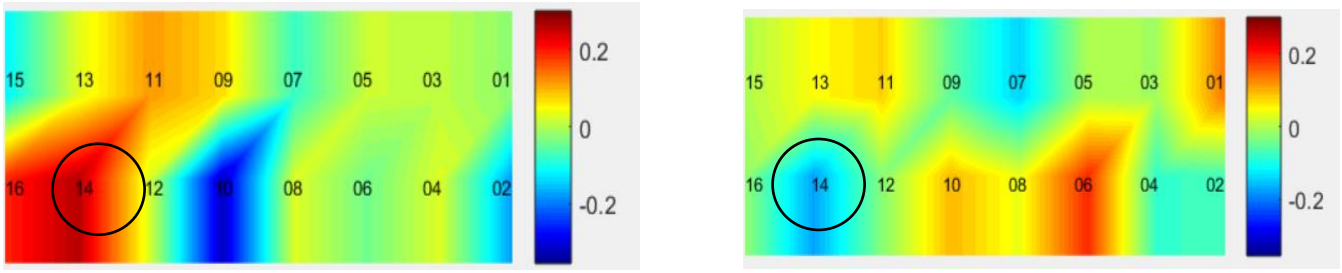

Figure 33: Young Vs Old: Hemodynamic Response of Go/No-Go

Figure (33) shows hemodynamic response comparison between healthy young & healthy old adults. For go & No-Go Condition, we could see bilateral activation in VLPFC for older adults and for younger adults there is mild deactivation in VLPFC. There were no significant channels for Go Task. But for No-Go task, channel 14 was significant. For Younger adults, activation was seen that is left lateralized. This could provide evidence that inhibitory control is related to ventrolateral Prefrontal region.

3.1.2.2 Cancer Vs Healthy Old

Healthy Old Cancer

Go condition

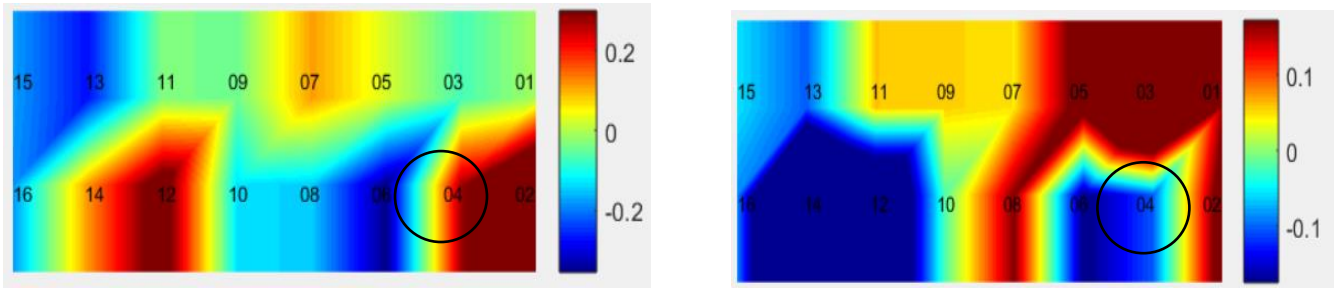

No-Go Condition

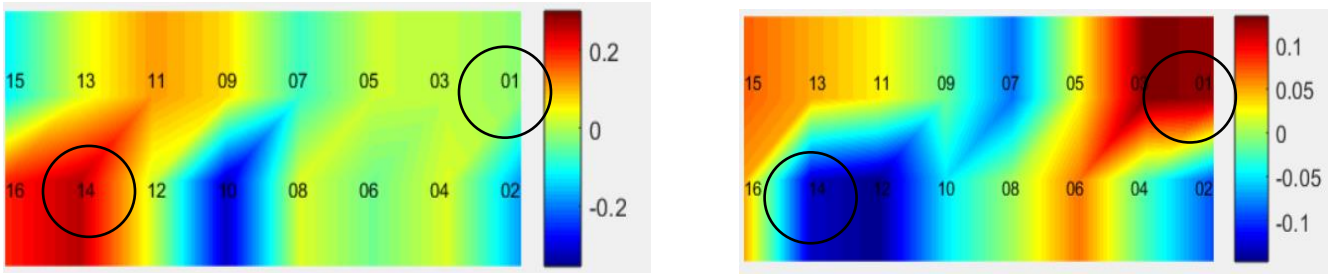

Figure 34: Cancer Vs healthy: Hemodynamic Response of Go/No-Go

Figure (34) shows hemodynamic response comparison between cancer & healthy adults. Here again, from the above figure, channel 14 was observed to be significant along with channel 1 for No-go and channel 4 for Go condition. Also, for cancer patients, more deactivation was observed in VLPFC when compared to healthy patients and more activation was observed in DLPFC for cancer survivors.

3.1.3. Hemodynamic Response: Stroop Test

The below figure (35) showed hemodynamic response of pre-frontal cortex for stroop task that measures cognitive flexibility between healthy older & young adults. The responses were measured for 120s baseline period and during 30-40s stroop stimuli with inter-block interval of 15-20 sec.

3.1.3.1 Healthy Old Vs Healthy Young

Old Young

Stroop 2

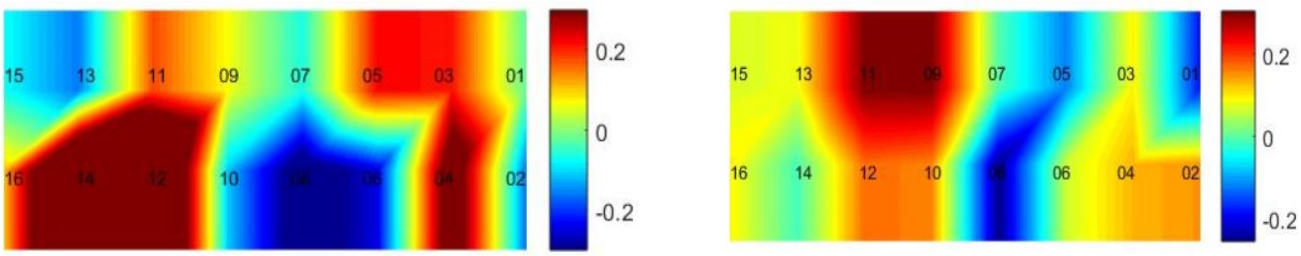

Stroop 3

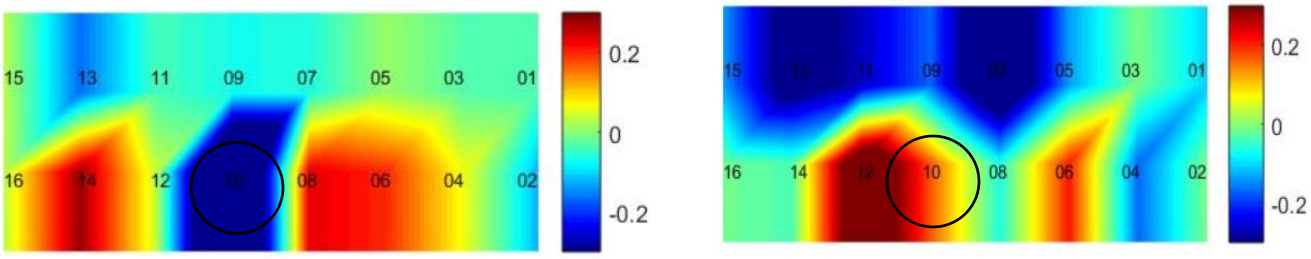

Figure 35: Healthy Vs Old: Hemodynamic Response of Stroop

Figure (35) shows hemodynamic response comparison between healthy young & healthy old adults. On performing two-sample t-test between healthy old and younger adults, out of 16 channels, single channel, channel 10 is found to be significant for stroop 3. For stroop, healthy older adults have shown bilateral VLPFC activation while younger adults have shown activation in right VLPFC and deactivation in DLPFC.

3.1.3.2 Cancer Vs Healthy Old

Healthy Old Cancer

Stroop 2

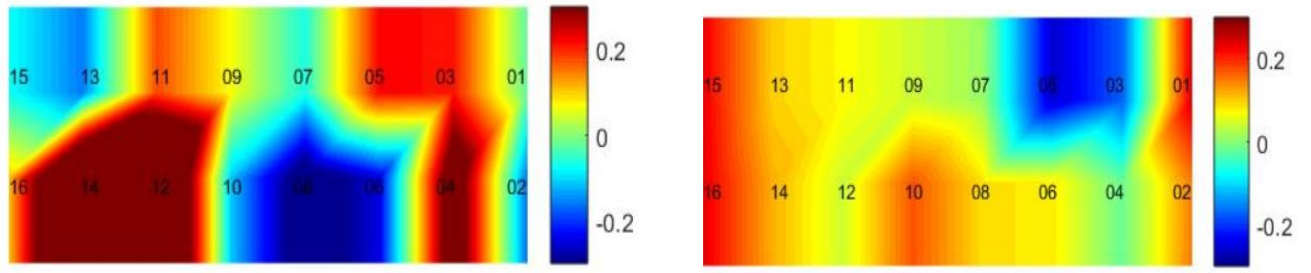

Stroop 3

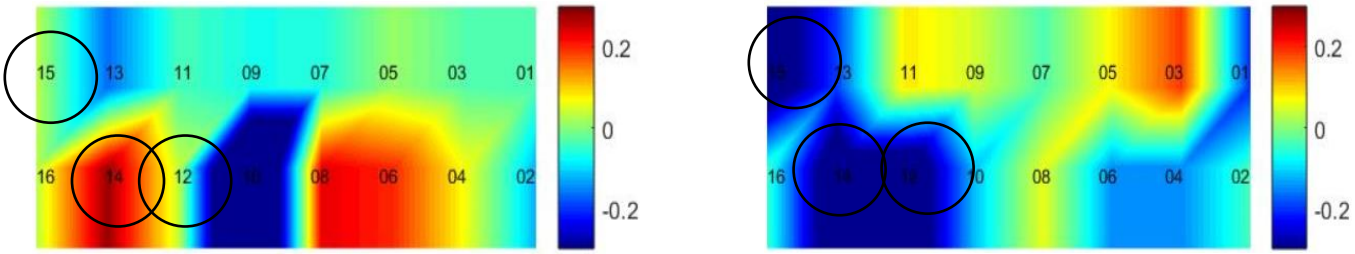

Figure 36: Cancer Vs Healthy Old: Hemodynamic response of Stroop

Figure (36) shows hemodynamic response comparison between cancer & healthy adults. On performing two-sample t-test between cancer and healthy adults, out of 16 channels, channel 12,14 & 16 were identified to be significantly different for cancer and healthy adults. And again, bilateral activation was observed for healthy adults, but there is deactivation in VLPFC for cancer subjects.

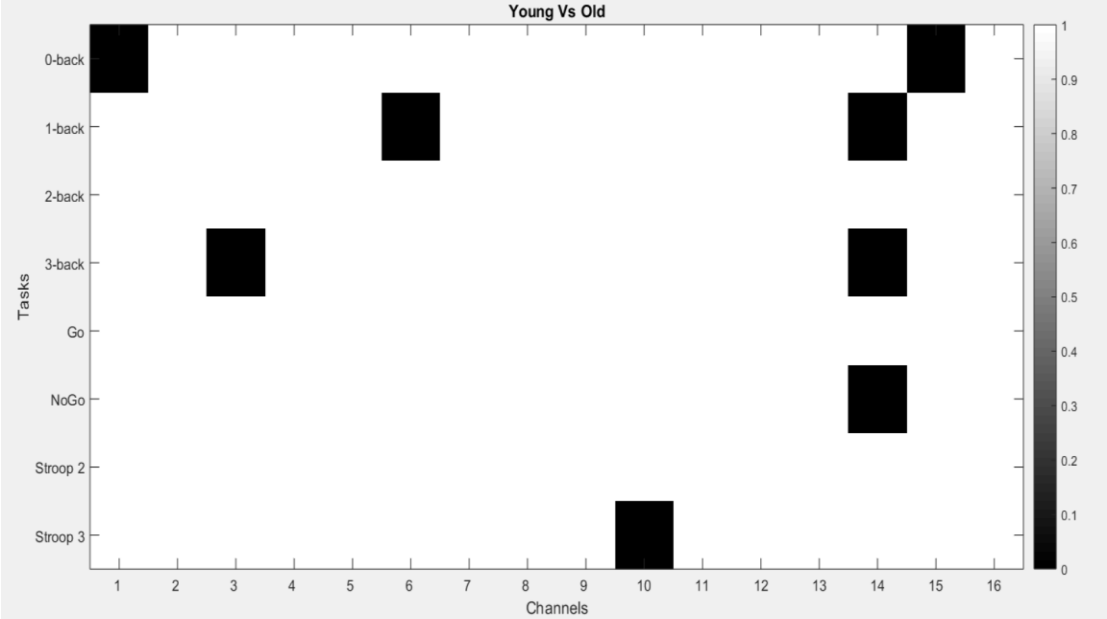

Figure 37: p-value plot: healthy old vs young

The above figure (37) shows the results for two-sample t-test for healthy old vs younger adults. P-values for each of the channels and for each task is plotted using MATLAB. The p-values were thresholded and

values less than 10% significance level (< 0.1) were made to be black color squared boxes. Channel 14 is found be consistently showing significant results for three tasks namely 1-back, 3-back & No-Go. Although, few other channels like channel 1, channel 3, channel 6 & 10 showed significant difference between healthy old and younger adults, most of the tasks have channel 14 to be significant. Also, channel 1 & 15 could not be considered as trustworthy as those channel locations are at the edges when doing interpolation.

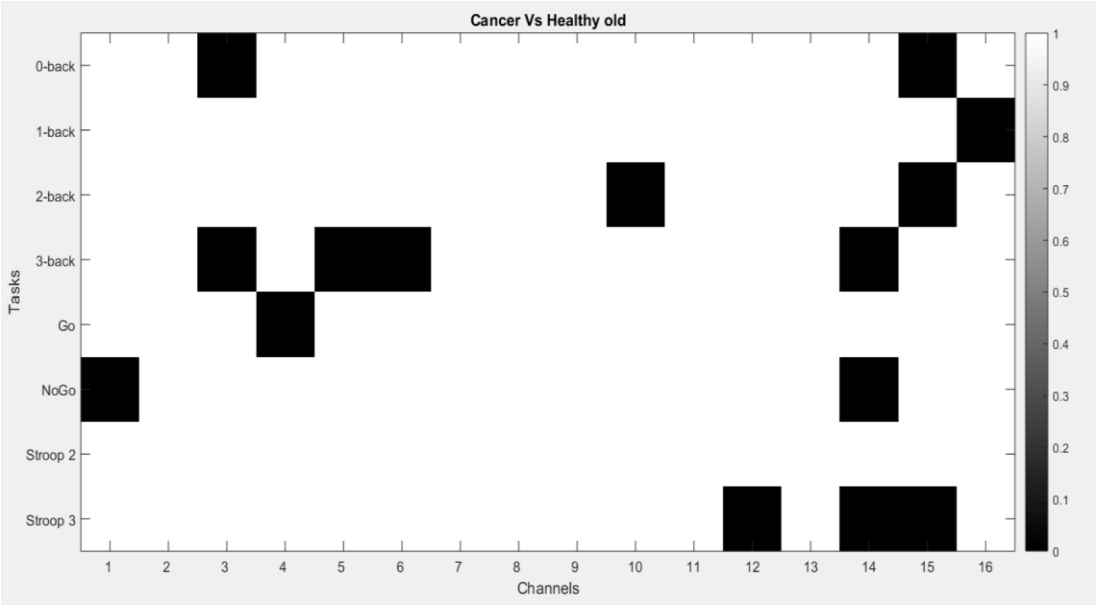

Figure 38: p-value plot : Cancer vs healthy old

The above figure (38) shows the results of to sample t-test between healthy old vs cancer patients. And the p-values were plotted for each channel and for each of the tasks. P-values less than 0.1 were plotted as black squared boxes. And again channel 14 in right VLPFC and channel 15 in right DLPFC were found to be significant for three different task. There were also few channels showing significance but not for many tasks. So, we can discard those channels and channel 1 and 16 were at the boundary and so we can exclude that also.

3.2 Statistical Results: Linear Mixed Effects Model

Table 4: Statistical Result: Linear Mixed Effect Model

Task	**Factors**	**Significance at 10%**
N-back	Age	-
	Gender	-
	Location	Ch2, Ch4, Ch6, Ch 8, Ch 16
	Task	-
Go/No-Go	Age	-
	Gender	-
	Location	-
	Task	-
Stroop	Age	-
	Gender	-
	Location	Ch 12, Ch 14
	Task	Yes

3.2.1 N-back Test:

For fitting linear mixed effect model, we have considered the effect of location, age, gender, task on the response variable 'Beta'. All the factors were taken together at a time. Location, age, gender, task were considered to show fixed effects and subjects were considered to be random as repeated measurements were taken from each subject for different tasks. Stroop 1 and 3-back were excluded from the study as data were not consistent. For, n-back, all the factors were turned out to be insignificant at 90 % confidence and only location effect turned out to be significant. Channel 2(p-value=0.004),4(p-value-0.003),6(p-value-0.003),16(p-value-0.004) were significant at 5% and channel 8 (p-value-0.022) at 10%

significance with location 1 as baseline. So, for n-back, these locations were identified to be significantly different from location 1 and has effect of increasing response or 'beta' values. Although we knew the locations, we did not know in which task it has shown significance and so we performed two-sample t-test.

3.2.2 Stroop test:

From the above table, factors gender & age have not turned out to be significant but locations and task were significant at 95 % confidence. So, Stroop 2 and stroop 3 were significantly different (p-value-0.044) with stroop 2 as baseline. Stroop 2 has more effect on response than stroop 3. Also, location has turned out to have significant effect on the response variable. Location 12 (p-value-0.018) was found to be significantly different from location 1 at 5% significance level and location 14 (p-value-0.088) was significant at 10% significance.

3.2.3 Go/No-Go test:

None of the factors have shown significant difference for G/No-Go task. All the factors age, gender, location, task turned out to be insignificant. Gender did not show any significant results because of less number of male subjects in both healthy old and younger adults. So, sample population might be one of the reason for gender to have shown non-significant effect on response.

Chapter-4

Discussion & Future Work

4.1 Discussion

Several previous studies have suggested that cognitive dysfunction may be the outcome of cancer related treatment in some cancer patients who received chemotherapy (10). It is of great concern to cancer patients what is referred to as “chemo-fog”. The majority of the previous studies were of patients with breast cancer and we have also concentrated on breast cancer patients because for the disease, rate of cognitive impairment is more. Cognitive decline is durable in some patients for few years even after the treatment. Previous studies have shown, patients who describe cognitive decline may perform within normal range on several neuropsychological tests because they might have performed at an elevated level before chemotherapy and have subtle decline in performance but still within normal range. Problems with memory and concentration were more evident when they resume their normal day-to-day work particularly with multi-tasking. Many studies have reported anatomical changes related to cognitive decline using MRI. But there were only few studies who have reported functional changes using minimally invasive method.

This study has evaluated the cognitive decline in cancer survivors and identified possible functional biomarker for CRND using optical imaging technique called fNIRs. This study also identified the differences between hemodynamic activation in healthy old controls and cancer survivors as well as old vs young subjects.

The main findings of this study are as follows:

1. This study demonstrated the feasibility of using FNIRS as a potential tool to study cognitive changes in cancer patients. For Young vs old healthy subjects, there was significant activation in the pre-frontal cortex. Healthy old adults have shown bilateral activation during all n-back conditions whereas younger adults showed slight right-hemispheric dominance during 0-back. Pre-frontal activity was found to be less lateralized in older adults to compensate for reduced neural efficiency and to match younger adults. They must recruit more cortical regions at higher memory load conditions. In case of young adults, at low-memory load they showed right

Table 5: Statistical Results: Two sample t-test healthy vs Young & Cancer vs Healthy

Tasks	Healthy Old Vs Cancer		Healthy Old Vs Young	
	Channels	Region	Channels	Region
N-back	3 6 10 15 16	L-DLPFC L-VLPFC MFC R-DLPFC R-VLPFC	1 3 6 14 15	L-DLPFC L-DLPFC L-VLPFC R-VLPFC R-DLPFC
Stroop	12 14 15	R-VLPFC R-VLPFC R-DLPFC	10	MFC
Go/No-Go	14	R-VLPFC	1 4 14	L-DLPFC L-VLPFC R-VLPFC

lateralization and at high task load, they started recruiting left hemisphere additionally which is in consistent with previous study done by Vermeij et al.,.

2. For Stroop and Go/No-Go also, bilateral activation was seen in older adults in order for them to compensate for age-related differences. For younger adults, activation was more lateralized towards right VLPFC as right inferior frontal gyrus or right-lateralized network is mainly involved in response inhibition and with high memory load.
3. For cancer patients, for all the tests, n-back, Go/No-Go and stroop have shown significant deactivation in right VLPFC which is involved in high memory load when normal controls have shown activation. On the contrary, DLPFC was shown to have slight activation. Few tasks have shown task related deactivation in DLPFC for normal control while task related deactivation in VLPFC for cancer subjects.
4. From the above table, statistical Tests have shown significant channels namely Channel 14 and channel 15 for three different tasks which could be taken as possible functional biomarker for studying age related changes and cancer/treatment related changes in cognitive function. As these channels correspond to VLPFC and DLPFC respectively, we can say that those regions play major role in working memory tasks. One possible explanation for DLPFC deactivation healthy controls would be, resting brain activity. During attention-requiring or goal directed tasks, DLPFC or MFC show deactivation. But Cancer groups did not show deactivation pattern in DLPFC which might indicate prefrontal deficits of default mode network (DMN) (11).

4.2 Limitations

This study had few limitations as described below:

1. This study was conducted with a very less sample size of 6 healthy older adults, 9 healthy younger adults & only 3 cancer patients due to which, it was difficult to determine difference in response between cancer and control, statistically.
2. Also, in this study, we did not have many male subjects which could have led to gender related bias which again might have affected statistical analysis.
3. The study was conducted only in the prefrontal regions which was too front believing that only those regions are involved in cognitive functions and ignored other brain regions.
4. For linear mixed effect model, as the model suggested we ought to choose one location as baseline and compared all other locations with respect to location 1 which itself might be activated or deactivated. Also, for other factors also, we have chosen one of the factor to be baseline and compared it with other.
5. This study demonstrated the hemodynamic response changes but accuracy i.e. how much correct responses were given by the patient or how much time they have taken to complete the task were not considered to account for hemodynamic changes.

4.3 Future Work

The above findings could be helpful to carry out this study towards future direction by considering the following factors:

1. In future, an increase in sample population for cancer as well as healthy old adults with comparable task paradigms could increase the probability of getting more accurate statistical results and also account for any statistical flaws in the current study.

2. We can extend this study to other regions of brain which are involved in attention or cognition for example, pre-SMA, parietal regions to evaluate the changes in functional network like default mode network and other network as few studies have reported changes in network due to cancer related cognitive decline.
3. We can also consider few factors like behavioral measures, reaction time, accuracy in order to see how hemodynamic response have changed with respect to behavioral measures and also to include pre-treatment, during and after treatment measures for effective comparison.

References

1. Ahles, T. A., & Saykin, A. J. (2007, March). Candidate mechanisms for chemotherapy-induced cognitive changes.
2. B.C. McDonald, S.K. Conroy, T.A. Ahles, J.D. West, A.J. Saykin. Alterations in brain activation during working memory processing associated with breast cancer and treatment: a prospective functional magnetic resonance imaging study. J. Clin. Oncol., 30 (20) (2012), pp. 2500–2508 (Jul 10)
3. Dietrich, J., Han, R., Yang, Y., Mayer-Pröschel, M., & Noble, M. (2006, November 30). CNS progenitor cells and oligodendrocytes are targets of chemotherapeutic agents in vitro and in vivo.
4. Duncan A, Meek JH, Clemence M, Elwell CE, Fallon P, et al. (1996) Measurement of cranial optical path length as a function of age using phase resolved near infrared spectroscopy. Pediatr Res 39: 889–894.
5. fNIR FAQ | BIOPAC. BIOPAC Systems, Inc. https://www.biopac.com/knowledge-base/fnir-faq/.
6. Hoshi Y, Tsou BH, Billock VA, Tanosaki M, Iguchi Y, et al. (2003b) Spatiotemporal characteristics of hemodynamic changes in the human lateral prefrontal cortex during working memory tasks. Neuroimage 20: 1493–1504.
7. Ian F. Tannock, Tim A. Ahles, Patricia A. Ganz, Frits S. van Dam . Cognitive Impairment Associated With Chemotherapy for Cancer: Report of a Workshop
8. ISS | Imagent: Functional Brain Imaging System. ISS | Imagent: Functional Brain Imaging System. http://www.iss.com/biomedical/instruments/imagent.html.

9. Jean-Pierre, P. (2014). Integrating functional near-infrared spectroscopy in the characterization, assessment, and monitoring of cancer and treatment-related neurocognitive dysfunction. NeuroImage,85, 408-414. doi:10.1016/j.neuroimage.2013.06.075
10. Jean-Pierre, P., Johnson-Greene, D., & Burish, T. G. (2014, March 27). Neuropsychological care and rehabilitation of cancer patients with chemobrain: strategies for evaluation and intervention development.
11. Len-Carrin J, Len-Domnguez U. Functional Near-Infrared Spectroscopy (fNIRS): Principles and Neuroscientific Applications. Neuroimaging - Methods. 2012. doi:10.5772/23146.
12. Liao L-D, Tsytsarev V, Delgado-Martínez I, et al. Neurovascular coupling: in vivo optical techniques for functional brain imaging. Published 2013.
13. Matsuda G, Hiraki K (2006) Sustained decrease in oxygenated hemoglobin during video games in the dorsal prefrontal cortex: a NIRS study of children. Neuroimage 29: 706–711.
Nat. Rev. Cancer, 7 (3) (2007), pp. 192–201
14. Owen AM, McMillan KM, Laird AR, Bullmore E (2005) N-back working memory paradigm: a meta-analysis of normative functional neuroimaging studies. Hum Brain Mapp 25: 46–59.
15. R.S. Scheibel, A.D. Valentine, S. O'Brien, C.A. Meyers. Cognitive dysfunction and depression during treatment with interferon-alpha and chemotherapy. J. Neuropsych. Clin. Neurosci., 16 (2004), pp. 185–191
16. S. Ancoli-Israel, L. Liu, M.R. Marler, B.A. Parker, V. Jones, G.R. Sadler, J. Dimsdale, M. Cohen-Zion, L. Fiorentino. Fatigue, sleep, and circadian rhythms prior to chemotherapy for breast cancer. Support. Care Cancer, 14 (2006), pp. 201–209
17. S. Deprez, F. Amant, A. Smeets, R. Peeters, A. Leemans, W. Van Hecke, J.S. Verhoeven, M.R. Christiaens, J. Vandenberghe, M. Vandenbulcke, S. Sunaert. Longitudinal assessment of

chemotherapy-induced structural changes in cerebral white matter and its correlation with impaired cognitive functioning. J. Clin. Oncol., 30 (3) (2012), pp. 274–281 (Jan 20)

18. Schroeter ML, Zysset S, Kruggel F, von Cramon DY (2003) Age dependency of the hemodynamic response as measured by functional near-infrared spectroscopy. Neuroimage 19: 555–564.
19. Shinsuke Koike, Ryu Takizawa, Yukkika Nishimura, Masaru Kinou, Shingo Kawasaki , Kiyoto Kasai. Reduced but broader prefrontal activity in patients with schizophrenia during n-back working memory tasks: A multi-channel near-infrared spectroscopy
20. T.A. Ahles, A.J. Saykin, B.C. McDonald, Y. Li, C.T. Furstenberg, B.S. Hanscom, T.J. Mulrooney, G.N. Schwartz, P.A. Kaufman. Longitudinal assessment of cognitive changes associated with adjuvant treatment for breast cancer: impact of age and cognitive reserve. J. Clin. Oncol., 28 (29) (2010), pp. 4434–4440
21. T.A. Ahles, A.J. Saykin. Candidate mechanisms for chemotherapy-induced cognitive changes
22. Torricelli, A., Contini, D., Mora, A. D., Pifferi, A., Re, R., Zucchelli, L., . . . Spinelli, L. (2014). Neurophotonics: non-invasive optical techniques for monitoring brain functions.
23. Vermeij, A., Arenda H. E. A. van Beek, Rikkert, M. G., Claassen, J. A., & Kessels, R. P. (2012). Effects of Aging on Cerebral Oxygenation during Working-Memory Performance: A Functional Near-Infrared Spectroscopy Study.